STATISTICS, OPTIMIZATION AND INFORMATION COMPUTING
Stat., Optim. Inf. Comput., Vol. **x**, Month 202x, pp 0–22.
Published online in International Academic Press (www.IAPress.org)

Optimal control of a fractional two-strain epidemic model with general incidence rates

Mohsine Aarir[1*], Sanaa Harroudi[1,2], Jaouad Danane[3], Karam Allali[1]

[1] *Laboratory of Mathematics, Computer Science and Applications, Faculty of Sciences and Technologies, University Hassan II of Casablanca, PO Box 146, Mohammedia, 20650, Morocco*
[2] *ENCG of Casablanca, University Hassan II, Casablanca, 20000, Morocco*
[3] *Laboratory of Systems Modelization and Analysis for Decision Support, National School of Applied Sciences, Hassan First University, Berrechid, 26100, Morocco*

Abstract We study a fractional-order two-strain $\mathcal{SI}_1\mathcal{I}_2\mathcal{R}$ epidemic model with general incidence functions, incorporating optimal control strategies for each infectious class. The system consists of four fractional differential equations describing the evolution of the susceptible population, two infected populations and the recovered population, and is formulated in terms of Caputo fractional derivatives. The existence, uniqueness, positivity and boundedness of solutions are established. The basic reproduction numbers are derived and the stability properties of the equilibria are investigated. An optimal control problem is then formulated by introducing two time-dependent control functions aimed at reducing the infection levels while minimizing the associated implementation costs. Using Pontryagin's Maximum Principle, the necessary optimality conditions are derived and the optimal controls are characterized. Numerical simulations illustrate the effectiveness of the proposed strategies: Optimal interventions substantially reduce the infection peaks and improve disease mitigation. Moreover, the fractional-order dynamics highlight the role of memory effects in shaping the epidemic behaviour.

Keywords Fractional-order model, Two-strain epidemic, General incidence, fractional optimal control, Caputo derivative, Lyapunov stability, Pontryagin Maximum Principle

AMS 2010 subject classifications 26A33, 37M05, 92B10, 34D23, 93D05

DOI: 10.19139/soic-2310-5070-4140

1. Introduction

Multi-strain epidemic models are key tools for studying the spread and evolution of infectious diseases with multiple variants. Many pathogens, including tuberculosis [38], human immunodeficiency virus (HIV) [4, 5, 7, 18, 35], COVID-19 [15, 24], hepatitis B virus (HBV) [14, 16, 42] and hepatitis C virus (HCV) [13, 29, 36, 37], circulate as several coexisting strains whose interaction strongly influences transmission dynamics and control strategies [6,41,43]. Consequently, multi-strain compartmental models have been extensively developed to capture the interactions between competing strains and to evaluate the effectiveness of intervention policies [11, 12, 44]. $\mathcal{SIR}$-type models remain highly relevant for directly transmitted diseases whose latent period is negligible or can be neglected. When several strains circulate, the infected class is split into subclasses, each associated with one strain, which leads to the $\mathcal{SI}_1\mathcal{I}_2\mathcal{R}$ structure considered here. The classical $\mathcal{SIR}$ model, introduced by Kermack and McKendrick in 1927 [22], provides the basis for analyzing key epidemiological quantities such as the basic reproduction number, the peak infection level and the herd immunity threshold. Over the years, this framework has been extended to incorporate multiple strains, nonlinear transmission mechanisms

*Correspondence to: Mohsine Aarir (Email: aarir.mohsine91@gmail.com). Laboratory of Mathematics, Computer Science and Applications, Faculty of Sciences and Technologies, University Hassan II of Casablanca, PO Box 146, Mohammedia, 20650, Morocco.

ISSN 2310-5070 (online) ISSN 2311-004X (print)

and optimal control strategies [9, 19, 21, 28, 33]. More recently, it has been applied to a variety of infectious diseases: Alfiniyah et al. [2] analyzed a Lassa fever model combining lockdown and treatment interventions, while Qomarudin et al. [34] investigated the spatial spread of an influenza virus in a bird population through a reaction–diffusion formulation. A crucial component of any epidemic model is the incidence function, which describes how susceptible individuals acquire the infection. The bilinear form $\beta\mathcal{S}\mathcal{I}$ remains the most widely used [8], but it does not account for saturation effects, behavioural responses or a limited contact rate. More general nonlinear incidence functions have therefore been introduced. In the present work we adopt the general forms $f(\mathcal{S},\mathcal{I}_1)\mathcal{I}_1$ and $h(\mathcal{S},\mathcal{I}_2)\mathcal{I}_2$, which cover a broad class of transmission mechanisms, including saturated and non-monotone incidences. Leaving the two functions unspecified and allowing them to differ from one strain to the other is what makes it possible to study competitive exclusion and coexistence within a single model, instead of fixing beforehand which strain is favoured by the choice of the incidence. Most classical epidemic models are formulated with integer-order differential equations, which cannot reproduce the memory and hereditary properties inherent in many biological systems. Fractional-order derivatives offer an alternative by incorporating such effects directly into the dynamics. The Caputo derivative, in particular, has been widely used in epidemiology to obtain a more realistic description of disease evolution [1, 17, 30, 31]. In the same direction, Tafrikan et al. [39] combined fractional dynamics and sensitivity analysis in a diphtheria spread model, showing that the sensitivity indices of the basic reproduction number provide valuable guidance for the design of control measures. Besides the description of the dynamics, the design of effective interventions is of paramount importance. Optimal control theory provides a systematic framework for determining time-dependent strategies that reduce the infection level while accounting for implementation costs. This motivates the introduction of two control functions representing the treatment effort applied to each infectious class.

Building on these considerations, we propose and analyze a fractional-order $\mathcal{S}\mathcal{I}_1\mathcal{I}_2\mathcal{R}$ epidemic model with general incidence functions and optimal control. The existence, positivity and boundedness of solutions are established. The basic reproduction number associated with each strain is derived and the stability of the equilibria is investigated by means of Lyapunov functionals. An optimal control problem is then formulated in order to minimize the number of infected individuals together with the cost of the interventions; the necessary optimality conditions are obtained from Pontryagin's Maximum Principle and the optimal controls are characterized. Numerical simulations illustrate the theoretical results and assess the impact of the proposed strategies. They show in particular that the fractional order does not modify the equilibrium reached by the system, but governs the speed at which it is approached, so that a population with strong memory experiences a flatter and longer epidemic wave than the integer-order model predicts.

Accordingly, the following system of fractional differential equations describes the proposed model:

$$\begin{cases} {}^{C}D_t^{\alpha}\mathcal{S}(t) = \lambda - (1-u_1)\, f(\mathcal{S},\mathcal{I}_1)\,\mathcal{I}_1 - (1-u_2)\, h(\mathcal{S},\mathcal{I}_2)\,\mathcal{I}_2 - \mu\,\mathcal{S}, \\ {}^{C}D_t^{\alpha}\mathcal{I}_1(t) = (1-u_1)\, f(\mathcal{S},\mathcal{I}_1)\,\mathcal{I}_1 - (\sigma_1+\mu)\,\mathcal{I}_1, \\ {}^{C}D_t^{\alpha}\mathcal{I}_2(t) = (1-u_2)\, h(\mathcal{S},\mathcal{I}_2)\,\mathcal{I}_2 - (\sigma_2+\mu)\,\mathcal{I}_2, \\ {}^{C}D_t^{\alpha}\mathcal{R}(t) = \sigma_1\mathcal{I}_1 + \sigma_2\mathcal{I}_2 - \mu\,\mathcal{R}. \end{cases} \tag{1}$$

with initial conditions

$$\mathcal{S}_0 \geq 0, \quad \mathcal{I}_{1,0} \geq 0, \quad \mathcal{I}_{2,0} \geq 0, \quad \mathcal{R}_0 \geq 0.$$

with,

(H$_1$) $f, h \in C^1(\mathbb{R}_+^2, \mathbb{R}_+)$, with $f(0,\mathcal{I}_1) = h(0,\mathcal{I}_2) = 0, \forall\, \mathcal{I}_1, \mathcal{I}_2 \geq 0$;

(H$_2$) $\dfrac{\partial f}{\partial \mathcal{S}}(\mathcal{S},\mathcal{I}_1) \geq 0$, $\dfrac{\partial h}{\partial \mathcal{S}}(\mathcal{S},\mathcal{I}_2) \geq 0, \forall\, \mathcal{S} > 0, \forall\, \mathcal{I}_1, \mathcal{I}_2 \geq 0$;

(H$_3$) $\dfrac{\partial f}{\partial \mathcal{I}_1}(\mathcal{S},\mathcal{I}_1) \leq 0$, $\dfrac{\partial h}{\partial \mathcal{I}_2}(\mathcal{S},\mathcal{I}_2) \leq 0, \forall\, \mathcal{S} \geq 0, \mathcal{I}_1, \mathcal{I}_2 \geq 0$.

Table 1. Description of variables and parameters of the $\mathcal{SI}_1\mathcal{I}_2\mathcal{R}$ model

Symbol	Description
$\mathcal{S}(t)$	Susceptible population
$\mathcal{I}_1(t)$	Individuals infected with strain 1
$\mathcal{I}_2(t)$	Individuals infected with strain 2
$\mathcal{R}(t)$	Recovered population
λ	Recruitment rate
μ	Natural death rate
σ_1	Recovery rate of $\mathcal{I}_1$
σ_2	Recovery rate of $\mathcal{I}_2$
$f(\mathcal{S},\mathcal{I}_1)$	Incidence function for strain 1
$h(\mathcal{S},\mathcal{I}_2)$	Incidence function for strain 2

All the model (1) parameters are given in Fig. 1.

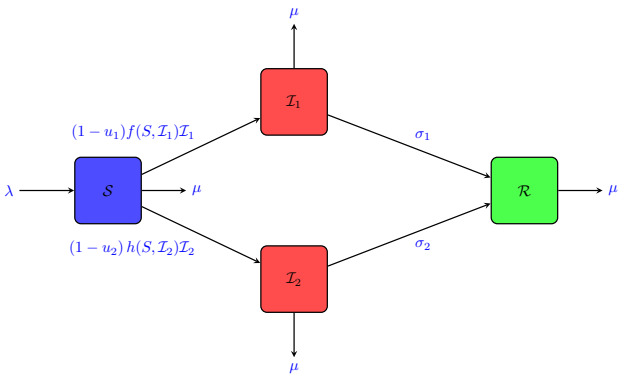

Figure 1. Flowchart of the fractional $\mathcal{SI}_1\mathcal{I}_2\mathcal{R}$ model with general incidence functions.

Table 2. Positioning of the present model with respect to representative multi-strain epidemic studies.

Reference	Order	Strains	Incidence	Control	Stability
Baba & Hincal [8]	integer	2	bilinear + non-monotone	no	global
Bentaleb et al. [11]	integer	multi	saturated	yes	global
Khyar & Allali [23]	integer	multi	general	no	global
Yaagoub et al. [41]	integer	2	specified	quarantine	global
Boukhouima et al. [12]	fractional	1	general	no	global
Tafrikan et al. [39]	fractional	1	specified	yes	local
Present work	fractional	2	general, strain-dependent	yes	global

Table 2 situates the present contribution. Fractional formulations with a general incidence exist, but for a single strain; two-strain models with a general incidence exist, but at integer order. What distinguishes the present setting is that the two incidence functions are left unspecified *and* are allowed to differ from one strain to the other. This is not a cosmetic generalisation, it produces competitive exclusion in a parameter regime where both reproduction numbers exceed unity, an outcome that models assigning a common functional form to both strains cannot exhibit.

The remainder of this paper is organized as follows. Section 2 introduces the fundamental concepts related to fractional derivatives. Section 3 establishes the existence and boundedness properties of the proposed model (1). In Section 4, the global stability of the equilibria associated with model (1) is analyzed. Section 5 presents the formulation and analysis of the corresponding optimal control problem. Numerical simulations and discussions, implemented using MATLAB, are provided in Section 6. The last section concludes the paper.

2. Preliminaries

Definition 1 (See Refs. [25, 32])
The Caputo fractional derivative of order $0 < \alpha < 1$ of a function $H \in C^1([0,\infty),\mathbb{R})$ is defined by

$$ {}^{C}D_t^{\alpha} H(t) = \left(I_{0^+}^{1-\alpha} H'\right)(t) = \frac{1}{\Gamma(1-\alpha)} \int_0^t \frac{H'(\tau)}{(t-\tau)^{\alpha}}\, d\tau, \tag{2} $$

where $I_{0^+}^{1-\alpha}$ denotes the Riemann–Liouville fractional integral of order $1-\alpha$, H' is the derivative of H with respect to time, and $\Gamma(z) = \int_0^{\infty} t^{z-1}e^{-t}\, dt$ is the Gamma function.

Lemma 1 (See Ref. [40])
Let $\psi(H) = H - \ln H - 1$ for $H \in \mathbb{R}_+^*$. Then, for every $0 < \alpha \leq 1$,

$$ {}^{C}D_t^{\alpha}\left[H_0\, \psi\left(\frac{H(t)}{H_0}\right)\right] \leq \left(1 - \frac{H_0}{H(t)}\right) {}^{C}D_t^{\alpha} H(t), \tag{3} $$

for any positive constant H_0 and any function H taking values in $\mathbb{R}_+^*$.

The LaSalle invariance principle is a standard tool for establishing the global stability of the equilibria of ordinary differential systems (see Refs. [10, 26]). Gallegos and Duarte-Mermoud [20] extended this principle to fractional-order systems with $0 < \alpha \leq 1$.

Theorem 2
Let x^* be an equilibrium point of a fractional-order differential system and let $F : V \to \mathbb{R}$ be defined on a neighbourhood $V \subset \mathbb{R}^n$ of x^*. If F satisfies

- F is continuously differentiable on $V \setminus \{x^*\}$;
- $F(x^*) = 0$;
- $F(x) > 0$ for all $x \in V \setminus \{x^*\}$;
- ${}^{C}D_t^{\alpha} F(x) \leq 0$ for all $x \in V \setminus \{x^*\}$, with $0 < \alpha \leq 1$;
- $\{x \in V : {}^{C}D_t^{\alpha} F(x) = 0\} = \{x^*\}$,

then x^* is globally asymptotically stable.

In order to establish the existence and uniqueness of solutions of system (1), we write it in the compact form

$$ {}^{C}D_t^{\alpha} X(t) = \mathcal{G}(X(t)), \qquad 0 < \alpha \leq 1, \tag{4} $$

with initial condition $X(0) = X_0 \in \mathbb{R}^n$.

Lemma 3 (See Ref. [27])
Assume that the function $\mathcal{G}$ satisfies the following conditions:

1. $\mathcal{G}(X)$ and $\dfrac{\partial \mathcal{G}}{\partial X}(X)$ are continuous on $\mathbb{R}^n$;
2. $\|\mathcal{G}(X)\| \leq q_1 + q_2\|X\|$ for all $X \in \mathbb{R}^n$, where q_1 and q_2 are positive constants.

Then system (4) admits a unique solution defined on $\mathbb{R}_+$.

3. Existence, positivity and boundedness

Since the state variables of model (1) represent population sizes, they must remain non-negative and bounded for the model to be biologically meaningful. In this section we establish these two properties, together with the existence and uniqueness of solutions. Throughout, the initial data are assumed to satisfy

$$\mathcal{S}(0) = \mathcal{S}_0 \geq 0, \quad \mathcal{I}_1(0) = \mathcal{I}_{1,0} \geq 0, \quad \mathcal{I}_2(0) = \mathcal{I}_{2,0} \geq 0, \quad \mathcal{R}(0) = \mathcal{R}_0 \geq 0.$$

Proposition 1
For any non-negative initial condition, system (1) admits a unique solution, which remains non-negative and bounded for all $t \geq 0$.

Proof
We first write system (1) in the compact vector form ${}^{C}D_t^{\alpha} X(t) = \mathcal{F}(X(t))$, where

$$X = \begin{pmatrix} \mathcal{S} \\ \mathcal{I}_1 \\ \mathcal{I}_2 \\ \mathcal{R} \end{pmatrix}, \qquad \mathcal{F}(X) = \begin{pmatrix} \lambda - (1-u_1) f(\mathcal{S},\mathcal{I}_1)\mathcal{I}_1 - (1-u_2) h(\mathcal{S},\mathcal{I}_2)\mathcal{I}_2 - \mu\mathcal{S} \\ (1-u_1) f(\mathcal{S},\mathcal{I}_1)\mathcal{I}_1 - (\sigma_1+\mu)\mathcal{I}_1 \\ (1-u_2) h(\mathcal{S},\mathcal{I}_2)\mathcal{I}_2 - (\sigma_2+\mu)\mathcal{I}_2 \\ \sigma_1\mathcal{I}_1 + \sigma_2\mathcal{I}_2 - \mu\mathcal{R} \end{pmatrix}.$$

By hypothesis (H_1), the functions f and h are continuously differentiable on $\mathbb{R}^2_+$, so that $\mathcal{F}$ and its Jacobian are continuous on $\mathbb{R}^4_+$; in particular $\mathcal{F}$ is locally Lipschitz. Lemma 3 then guarantees the existence of a unique local solution.

Non-negativity. On the faces of $\mathbb{R}^4_+$ the vector field points inwards. Indeed,

$$\begin{cases} {}^{C}D_t^{\alpha}\mathcal{S}\big|_{\mathcal{S}=0} = \lambda > 0, \\ {}^{C}D_t^{\alpha}\mathcal{I}_1\big|_{\mathcal{I}_1=0} = 0, \\ {}^{C}D_t^{\alpha}\mathcal{I}_2\big|_{\mathcal{I}_2=0} = 0, \\ {}^{C}D_t^{\alpha}\mathcal{R}\big|_{\mathcal{R}=0} = \sigma_1\mathcal{I}_1 + \sigma_2\mathcal{I}_2 \geq 0, \end{cases}$$

where we have used hypothesis (H_1), namely $f(0,\mathcal{I}_1) = h(0,\mathcal{I}_2) = 0$. Consequently, every trajectory starting in $\mathbb{R}^4_+$ remains in $\mathbb{R}^4_+$.

Boundedness. Let $\mathcal{N}(t) = \mathcal{S}(t) + \mathcal{I}_1(t) + \mathcal{I}_2(t) + \mathcal{R}(t)$. Adding the four equations of (1) gives

$${}^{C}D_t^{\alpha}\mathcal{N}(t) = \lambda - \mu\,\mathcal{N}(t),$$

whose solution is

$$\mathcal{N}(t) = \frac{\lambda}{\mu} + \left(\mathcal{N}(0) - \frac{\lambda}{\mu}\right) E_{\alpha}(-\mu t^{\alpha}),$$

where E_{α} denotes the one-parameter Mittag–Leffler function. Since $0 < E_{\alpha}(-\mu t^{\alpha}) \leq 1$ for every $t \geq 0$, we obtain

$$0 \leq \mathcal{N}(t) \leq \max\left\{\mathcal{N}(0),\ \frac{\lambda}{\mu}\right\}, \qquad \limsup_{t\to\infty} \mathcal{N}(t) \leq \frac{\lambda}{\mu}.$$

In particular, the region

$$\mathcal{H} = \left\{(\mathcal{S},\mathcal{I}_1,\mathcal{I}_2,\mathcal{R}) \in \mathbb{R}^4_+ : \mathcal{S}+\mathcal{I}_1+\mathcal{I}_2+\mathcal{R} \leq \frac{\lambda}{\mu}\right\}$$

is positively invariant and attracts all solutions. The solution is therefore bounded on its maximal interval of existence, which implies that this interval is $[0,\infty)$; uniqueness follows from the local Lipschitz continuity of $\mathcal{F}$ on the bounded set $\mathcal{H}$. □

4. The steady states

This section is devoted to the existence of the disease-free equilibrium and of the endemic equilibria of the fractional model. Since the variable $\mathcal{R}$ does not appear in the first three equations of (1), the steady states can be determined from the subsystem governing $(\mathcal{S}, \mathcal{I}_1, \mathcal{I}_2)$, namely

$$\begin{cases} {}^{C}D_t^{\alpha}\mathcal{S}(t) = \lambda - (1-u_1)f(\mathcal{S},\mathcal{I}_1)\mathcal{I}_1 - (1-u_2)h(\mathcal{S},\mathcal{I}_2)\mathcal{I}_2 - \mu\mathcal{S}, \\ {}^{C}D_t^{\alpha}\mathcal{I}_1(t) = (1-u_1)f(\mathcal{S},\mathcal{I}_1)\mathcal{I}_1 - (\sigma_1+\mu)\mathcal{I}_1, \\ {}^{C}D_t^{\alpha}\mathcal{I}_2(t) = (1-u_2)h(\mathcal{S},\mathcal{I}_2)\mathcal{I}_2 - (\sigma_2+\mu)\mathcal{I}_2, \end{cases} \tag{5}$$

the recovered population being recovered a posteriori from $\mathcal{R}(t) = \mathcal{N}(t) - \mathcal{S}(t) - \mathcal{I}_1(t) - \mathcal{I}_2(t)$, where $\mathcal{N}$ solves ${}^{C}D_t^{\alpha}\mathcal{N}(t) = \lambda - \mu\mathcal{N}(t)$.

4.1. The basic reproduction number

The basic reproduction number is the average number of secondary infections generated by a single infected individual introduced into a wholly susceptible population. We compute it by the next-generation matrix method. Denote by $\mathbb{F}$ the matrix of new infection terms and by V the matrix of transfer terms between the infected compartments of (5). Evaluated at the disease-free equilibrium $\mathcal{E}_f = \left(\frac{\lambda}{\mu}, 0, 0\right)$, these matrices read

$$\mathbb{F} = \begin{pmatrix} (1-u_1)\, f\left(\frac{\lambda}{\mu}, 0\right) & 0 \\ 0 & (1-u_2)\, h\left(\frac{\lambda}{\mu}, 0\right) \end{pmatrix}, \qquad V = \begin{pmatrix} \sigma_1+\mu & 0 \\ 0 & \sigma_2+\mu \end{pmatrix},$$

so that

$$\mathbb{F}V^{-1} = \begin{pmatrix} \dfrac{(1-u_1)f\left(\frac{\lambda}{\mu}, 0\right)}{\sigma_1+\mu} & 0 \\ 0 & \dfrac{(1-u_2)h\left(\frac{\lambda}{\mu}, 0\right)}{\sigma_2+\mu} \end{pmatrix}.$$

The basic reproduction number is the spectral radius of $\mathbb{F}V^{-1}$,

$$R_0 = \max\{R_{0,1},\ R_{0,2}\}, \qquad R_{0,i} = \frac{(1-u_i)\, g_i\left(\frac{\lambda}{\mu}, 0\right)}{\sigma_i+\mu}, \quad i = 1, 2,$$

where $g_1 = f$ and $g_2 = h$. The quantities $R_{0,1}$ and $R_{0,2}$ are the reproduction numbers of the first and of the second strain. If $R_0 < 1$, both strains die out; if $R_0 > 1$, at least one of them can invade the population. When a single threshold exceeds unity, the corresponding strain excludes the other, whereas coexistence becomes possible when both do.

Theorem 4
System (5) always admits the disease-free equilibrium $\mathcal{E}_f$. Moreover:

- a strain–1 endemic equilibrium $\mathcal{E}_{s_1}$ exists if and only if $R_{0,1} > 1$;
- a strain–2 endemic equilibrium $\mathcal{E}_{s_2}$ exists if and only if $R_{0,2} > 1$;
- a coexistence equilibrium $\mathcal{E}_{s_t}$ may exist only if $R_{0,1} > 1$ and $R_{0,2} > 1$.

Proof
The steady states are the solutions of

$$\begin{cases} 0 = \lambda - (1-u_1) f(\mathcal{S},\mathcal{I}_1)\mathcal{I}_1 - (1-u_2) h(\mathcal{S},\mathcal{I}_2)\mathcal{I}_2 - \mu\mathcal{S}, \\ 0 = (1-u_1) f(\mathcal{S},\mathcal{I}_1)\mathcal{I}_1 - (\sigma_1+\mu)\mathcal{I}_1, \\ 0 = (1-u_2) h(\mathcal{S},\mathcal{I}_2)\mathcal{I}_2 - (\sigma_2+\mu)\mathcal{I}_2, \\ 0 = \sigma_1\mathcal{I}_1 + \sigma_2\mathcal{I}_2 - \mu\mathcal{R}. \end{cases} \tag{6}$$

1. *Disease-free equilibrium.* Taking $\mathcal{I}_1 = \mathcal{I}_2 = 0$ in (6) yields at once $\mathcal{E}_f = \left(\frac{\lambda}{\mu}, 0, 0, 0\right)$.

2. *Strain–1 endemic equilibrium.* Let $\mathcal{I}_1 > 0$ and $\mathcal{I}_2 = 0$. Dividing the second equation of (6) by $\mathcal{I}_1$ gives

$$(1-u_1) f(\mathcal{S},\mathcal{I}_1) = \sigma_1 + \mu,$$

and substituting this relation into the first equation yields $\lambda - \mu\mathcal{S} = (\sigma_1+\mu)\mathcal{I}_1$, that is $\mathcal{I}_1 = \phi(\mathcal{S})$ with

$$\phi(\mathcal{S}) := \frac{\lambda - \mu\mathcal{S}}{\sigma_1+\mu}, \qquad \phi'(\mathcal{S}) = -\frac{\mu}{\sigma_1+\mu} < 0. \tag{7}$$

Note that $\phi(\mathcal{S}) \geq 0$ precisely when $\mathcal{S} \leq \frac{\lambda}{\mu}$, so we may restrict the analysis to the interval $[0, \frac{\lambda}{\mu}]$. Define $\Psi : [0, \frac{\lambda}{\mu}] \to \mathbb{R}$ by

$$\Psi(\mathcal{S}) := (1-u_1)\, f(\mathcal{S}, \phi(\mathcal{S})) - (\sigma_1+\mu). \tag{8}$$

A root of Ψ in $(0, \lambda/\mu)$ corresponds to a strain–1 endemic equilibrium, and conversely. Differentiating (8) and using (7),

$$\Psi'(\mathcal{S}) = (1-u_1)\left[\frac{\partial f}{\partial \mathcal{S}}(\mathcal{S},\phi(\mathcal{S})) - \frac{\mu}{\sigma_1+\mu}\,\frac{\partial f}{\partial \mathcal{I}_1}(\mathcal{S},\phi(\mathcal{S}))\right]. \tag{9}$$

By (H_2) the first term inside the brackets is non-negative, and by (H_3) the second one is non-negative as well, since it is preceded by a minus sign; hence $\Psi'(\mathcal{S}) \geq 0$ on $[0, \frac{\lambda}{\mu}]$, so that Ψ is non-decreasing.
At the endpoints, hypothesis (H_1) gives $f(0,\cdot) = 0$, whence

$$\Psi(0) = -(\sigma_1+\mu) < 0, \qquad \Psi\left(\frac{\lambda}{\mu}\right) = (1-u_1) f\left(\frac{\lambda}{\mu}, 0\right) - (\sigma_1+\mu) = (\sigma_1+\mu)\,(R_{0,1}-1)\,.$$

If $R_{0,1} > 1$, then $\Psi(\lambda/\mu) > 0$; being continuous and non-decreasing, Ψ vanishes at a unique point $\mathcal{S}_1^* \in (0, \frac{\lambda}{\mu})$. The corresponding equilibrium is

$$\mathcal{E}_{s_1} = \left(\mathcal{S}_1^*,\ \mathcal{I}_1^*,\ 0,\ \frac{\sigma_1\mathcal{I}_1^*}{\mu}\right), \qquad \mathcal{I}_1^* = \frac{\lambda - \mu\mathcal{S}_1^*}{\sigma_1+\mu} > 0.$$

Conversely, if $R_{0,1} \leq 1$ then $\Psi \leq 0$ on the whole interval and vanishes only possibly at $\mathcal{S} = \frac{\lambda}{\mu}$, where $\mathcal{I}_1 = 0$; no endemic equilibrium exists.

3. *Strain–2 endemic equilibrium.* Let now $\mathcal{I}_2 > 0$ and $\mathcal{I}_1 = 0$. The same argument applied to the third equation of (6) gives

$$(1-u_2) h(\mathcal{S},\mathcal{I}_2) = \sigma_2 + \mu, \qquad \mathcal{I}_2 = \frac{\lambda - \mu\mathcal{S}}{\sigma_2+\mu},$$

and leads to the function

$$\Phi(\mathcal{S}) := (1-u_2)\,h\left(\mathcal{S}, \frac{\lambda-\mu\mathcal{S}}{\sigma_2+\mu}\right) - (\sigma_2+\mu), \qquad \mathcal{S}\in[0,\frac{\lambda}{\mu}],$$

which is non-decreasing by (H_2)–(H_3) and satisfies

$$\Phi(0) = -(\sigma_2+\mu) < 0, \qquad \Phi\left(\frac{\lambda}{\mu}\right) = (\sigma_2+\mu)(R_{0,2}-1).$$

Hence, if and only if $R_{0,2}>1$, there is a unique $\mathcal{S}_2^*\in(0,\lambda/\mu)$ with $\Phi(\mathcal{S}_2^*)=0$, which yields the strain–2 endemic equilibrium

$$\mathcal{E}_{s_2} = \left(\mathcal{S}_2^*,\ 0,\ \mathcal{I}_2^*,\ \frac{\sigma_2\mathcal{I}_2^*}{\mu}\right), \qquad \mathcal{I}_2^* = \frac{\lambda-\mu\mathcal{S}_2^*}{\sigma_2+\mu} > 0.$$

4. *Coexistence equilibrium.* Suppose finally $\mathcal{I}_1>0$ and $\mathcal{I}_2>0$. The second and third equations of (6) then impose simultaneously

$$(1-u_1)f(\mathcal{S},\mathcal{I}_1) = \sigma_1+\mu, \qquad (1-u_2)h(\mathcal{S},\mathcal{I}_2) = \sigma_2+\mu, \tag{10}$$

while the first equation reduces to

$$(\sigma_1+\mu)\mathcal{I}_1 + (\sigma_2+\mu)\mathcal{I}_2 = \lambda-\mu\mathcal{S}.$$

A necessary condition for such a solution to exist is $R_{0,1}>1$ and $R_{0,2}>1$: indeed, by (H_2) and (H_3), $f(\mathcal{S},\mathcal{I}_1)\le f(\frac{\lambda}{\mu},0)$ for every admissible pair, so the first identity in (10) forces $(1-u_1)f(\frac{\lambda}{\mu},0)\ge\sigma_1+\mu$, and similarly for the second strain. Whether this condition is also sufficient depends on the specific form of f and h; the two identities in (10) define two curves in the $(\mathcal{S},\mathcal{I}_1)$ and $(\mathcal{S},\mathcal{I}_2)$ planes, and coexistence requires them to be compatible with the conservation relation above.

□

4.2. Sensitivity analysis

To identify the parameters that most strongly influence the transmission dynamics, we perform a sensitivity analysis of the basic reproduction numbers $R_{0,1}$ and $R_{0,2}$ with respect to the model parameters. The normalized forward sensitivity index of a quantity R with respect to a parameter p is defined by

$$\Upsilon_p^R = \frac{\partial R}{\partial p}\frac{p}{R}.$$

This index measures the relative variation of R induced by a relative variation of p: a value $\Upsilon_p^R=1$ means that a 1% increase of p produces a 1% increase of R, while a negative index indicates an inverse relationship. Such indices have been widely used in recent epidemiological studies to rank the influence of the model parameters [39].

For illustration, we consider the incidence functions used in the numerical section, $f(\mathcal{S},\mathcal{I}_1)=\dfrac{\beta_1\mathcal{S}}{1+m\mathcal{I}_1^2}$ and $h(\mathcal{S},\mathcal{I}_2)=\beta_2\mathcal{S}$, so that

$$R_{0,1} = \frac{(1-u_1)\,\beta_1\lambda}{\mu(\sigma_1+\mu)}, \qquad R_{0,2} = \frac{(1-u_2)\,\beta_2\lambda}{\mu(\sigma_2+\mu)}.$$

A direct computation gives, for $i=1,2$,

$$\Upsilon_{\beta_i}^{R_{0,i}} = 1, \qquad \Upsilon_{\lambda}^{R_{0,i}} = 1, \qquad \Upsilon_{\sigma_i}^{R_{0,i}} = -\frac{\sigma_i}{\sigma_i+\mu},$$

$$\Upsilon_{\mu}^{R_{0,i}} = -\Big(1 + \frac{\mu}{\sigma_i + \mu}\Big), \qquad \Upsilon_{u_i}^{R_{0,i}} = -\frac{u_i}{1 - u_i}.$$

Parameter	$\Upsilon_p^{R_{0,1}}$	$\Upsilon_p^{R_{0,2}}$
λ	1	1
β_i	1	1
σ_i	-0.43	-0.43
μ	-1.57	-1.57
u_i	-0.25	-0.25

Table 3. Normalized sensitivity indices of $R_{0,1}$ and $R_{0,2}$ evaluated at $\lambda = 1$, $\beta_1 = \beta_2 = 0.6$, $\sigma_1 = \sigma_2 = 0.15$, $\mu = 0.2$, $u_1 = u_2 = 0.2$.

Table 3 and Fig. 2 show that the recruitment rate λ and the transmission rates β_1, β_2 have positive indices equal to unity, so any increase of these parameters directly amplifies the epidemic. Conversely, the natural death rate μ exhibits the largest index in absolute value, followed by the recovery rates σ_i and the controls u_i, whose negative indices confirm that treatment efforts reduce the reproduction numbers. This analysis indicates that intervention policies acting on β_i and u_i are the most efficient levers to bring $R_{0,i}$ below unity.

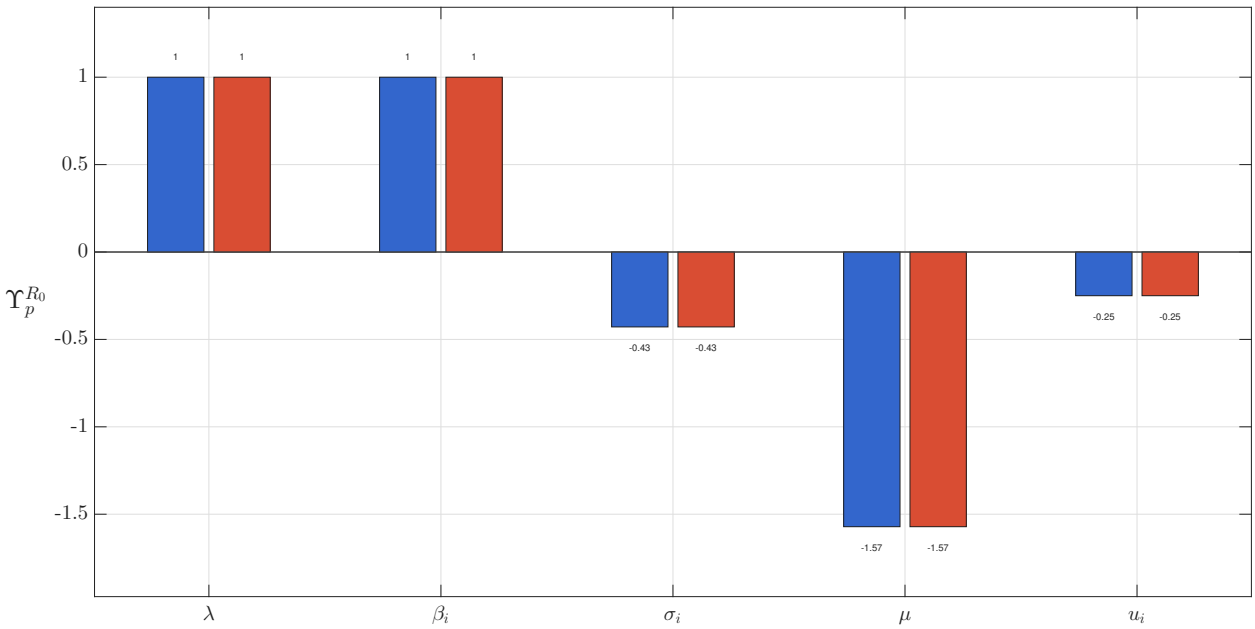

Figure 2. Normalized forward sensitivity indices of the basic reproduction numbers $R_{0,1}$ and $R_{0,2}$ with respect to the model parameters.

4.3. Global stability of equilibria

4.3.1. Global stability of the disease-free equilibrium

Theorem 5
If $R_{0,1} \leq 1$ and $R_{0,2} \leq 1$, then the disease-free equilibrium $\mathcal{E}_f$ is globally asymptotically stable.

Proof

Set $\mathcal{S}^0 = \dfrac{\lambda}{\mu}$ and consider the Lyapunov functional

$$\mathcal{P}_0(\mathcal{S},\mathcal{I}_1,\mathcal{I}_2) = \mathcal{S} - \mathcal{S}^0 - \int_{\mathcal{S}^0}^{\mathcal{S}} \frac{f(\mathcal{S}^0,0)}{f(X,0)}\,dX \;+\; \mathcal{I}_1 + \mathcal{I}_2.$$

The integral is well defined since, by (H_1) and (H_2), the map $X \mapsto f(X,0)$ is continuous and positive for $X > 0$. Moreover $\mathcal{P}_0 \geq 0$ on the interior of $\mathcal{H}$ and vanishes only at $\mathcal{E}_f$. Applying Lemma 1 and to each term and differentiating along the solutions of (1), we obtain

$$\begin{aligned}
{}^{C}D_t^{\alpha}\mathcal{P}_0 &\leq \left(1 - \frac{f(\mathcal{S}^0,0)}{f(\mathcal{S},0)}\right) {}^{C}D_t^{\alpha}\mathcal{S} \;+\; {}^{C}D_t^{\alpha}\mathcal{I}_1 \;+\; {}^{C}D_t^{\alpha}\mathcal{I}_2 \\
&= \left(1 - \frac{f(\mathcal{S}^0,0)}{f(\mathcal{S},0)}\right)\Big(\lambda - (1-u_1)f(\mathcal{S},\mathcal{I}_1)\mathcal{I}_1 - (1-u_2)h(\mathcal{S},\mathcal{I}_2)\mathcal{I}_2 - \mu\mathcal{S}\Big) \\
&\quad + (1-u_1)f(\mathcal{S},\mathcal{I}_1)\mathcal{I}_1 - (\sigma_1+\mu)\mathcal{I}_1 + (1-u_2)h(\mathcal{S},\mathcal{I}_2)\mathcal{I}_2 - (\sigma_2+\mu)\mathcal{I}_2.
\end{aligned}$$

Using $\lambda = \mu\mathcal{S}^0$ and regrouping the terms according to $\mathcal{I}_1$ and $\mathcal{I}_2$ yields

$$\begin{aligned}
{}^{C}D_t^{\alpha}\mathcal{P}_0 \leq \mu\mathcal{S}^0 &\left(1 - \frac{\mathcal{S}}{\mathcal{S}^0}\right)\left(1 - \frac{f(\mathcal{S}^0,0)}{f(\mathcal{S},0)}\right) \\
&+ \mathcal{I}_1\left\{(1-u_1)\,\frac{f(\mathcal{S}^0,0)}{f(\mathcal{S},0)}\,f(\mathcal{S},\mathcal{I}_1) - (\sigma_1+\mu)\right\} \\
&+ \mathcal{I}_2\left\{(1-u_2)\,\frac{f(\mathcal{S}^0,0)}{f(\mathcal{S},0)}\,h(\mathcal{S},\mathcal{I}_2) - (\sigma_2+\mu)\right\}.
\end{aligned}$$

In terms of the reproduction numbers

$$R_{0,1} = \frac{(1-u_1)f(\mathcal{S}^0,0)}{\sigma_1+\mu}, \qquad R_{0,2} = \frac{(1-u_2)h(\mathcal{S}^0,0)}{\sigma_2+\mu},$$

this reads

$$\begin{aligned}
{}^{C}D_t^{\alpha}\mathcal{P}_0 \leq \mu\mathcal{S}^0 &\left(1 - \frac{\mathcal{S}}{\mathcal{S}^0}\right)\left(1 - \frac{f(\mathcal{S}^0,0)}{f(\mathcal{S},0)}\right) \\
&+ (\sigma_1+\mu)\,\mathcal{I}_1\left(R_{0,1}\,\frac{f(\mathcal{S},\mathcal{I}_1)}{f(\mathcal{S},0)} - 1\right) \\
&+ (\sigma_2+\mu)\,\mathcal{I}_2\left(R_{0,2}\,\frac{h(\mathcal{S},\mathcal{I}_2)}{h(\mathcal{S}^0,0)}\cdot\frac{f(\mathcal{S}^0,0)}{f(\mathcal{S},0)} - 1\right).
\end{aligned} \tag{11}$$

We now bound each of the three contributions.

First term. By (H_2) the function $X \mapsto f(X,0)$ is non-decreasing. If $\mathcal{S} \leq \mathcal{S}^0$, then $1 - \dfrac{\mathcal{S}}{\mathcal{S}^0} \geq 0$ while $1 - \dfrac{f(\mathcal{S}^0,0)}{f(\mathcal{S},0)} \leq 0$; if $\mathcal{S} > \mathcal{S}^0$, both signs are reversed. In either case the product is non-positive:

$$\mu\mathcal{S}^0\left(1 - \frac{\mathcal{S}}{\mathcal{S}^0}\right)\left(1 - \frac{f(\mathcal{S}^0,0)}{f(\mathcal{S},0)}\right) \leq 0.$$

Second term. Hypothesis (H_3) states that f is non-increasing with respect to its second argument, hence $f(\mathcal{S},\mathcal{I}_1) \leq f(\mathcal{S},0)$ and

$$\frac{f(\mathcal{S},\mathcal{I}_1)}{f(\mathcal{S},0)} \leq 1.$$

Consequently, if $R_{0,1} \le 1$,

$$(\sigma_1+\mu)\,\mathcal{I}_1\left(R_{0,1}\,\frac{f(\mathcal{S},\mathcal{I}_1)}{f(\mathcal{S},0)}-1\right) \le (\sigma_1+\mu)\,\mathcal{I}_1\,(R_{0,1}-1) \le 0.$$

Third term. By (H_2) and (H_3), $h(\mathcal{S},\mathcal{I}_2) \le h(\mathcal{S},0)$ and, on the invariant region $\mathcal{H}$, $\mathcal{S} \le \mathcal{S}^0$, so that $h(\mathcal{S},0) \le h(\mathcal{S}^0,0)$ and $f(\mathcal{S}^0,0)/f(\mathcal{S},0) \ge 1$. A short computation shows that the product of these two ratios is bounded above by $f(\mathcal{S}^0,0)/f(\mathcal{S},0)$, which tends to 1 as $\mathcal{S} \to \mathcal{S}^0$. Hence, if $R_{0,2} \le 1$,

$$(\sigma_2+\mu)\,\mathcal{I}_2\left(R_{0,2}\,\frac{h(\mathcal{S},\mathcal{I}_2)}{h(\mathcal{S}^0,0)}\cdot\frac{f(\mathcal{S}^0,0)}{f(\mathcal{S},0)}-1\right) \le 0.$$

Collecting the three estimates in (11), we conclude that ${}^{C}D_t^{\alpha}\mathcal{P}_0 \le 0$ whenever $R_{0,1} \le 1$ and $R_{0,2} \le 1$. Equality forces $\mathcal{S}=\mathcal{S}^0$ and $\mathcal{I}_1=\mathcal{I}_2=0$, so that the largest invariant set contained in $\{{}^{C}D_t^{\alpha}\mathcal{P}_0=0\}$ reduces to $\{\mathcal{E}_f\}$. By the fractional LaSalle invariance principle (Theorem 2.3), $\mathcal{E}_f$ is globally asymptotically stable. □

4.3.2. Global stability of the strain-1 endemic equilibrium

Theorem 6
If $R_{0,2} \le 1 < R_{0,1}$, then the strain–1 endemic equilibrium $\mathcal{E}_{s_1}$ is globally asymptotically stable.

Proof
Write $\mathcal{E}_{s_1} = (\mathcal{S}_1^*,\, \mathcal{I}_1^*,\, 0,\, \mathcal{R}_1^*)$ for brevity. This equilibrium satisfies

$$(1-u_1)f(\mathcal{S}_1^*,\mathcal{I}_1^*) = \sigma_1+\mu, \qquad \lambda = \mu\,\mathcal{S}_1^* + (1-u_1)f(\mathcal{S}_1^*,\mathcal{I}_1^*)\,\mathcal{I}_1^*, \qquad \mu\,\mathcal{R}_1^* = \sigma_1\mathcal{I}_1^*. \tag{12}$$

Since the fourth equation of (1) is decoupled from the first three, it suffices to prove the result for the reduced system (5); the convergence of $\mathcal{R}$ to $\mathcal{R}_1^*$ then follows from the third relation in (12).

Consider the Lyapunov functional

$$\begin{aligned}\mathcal{P}_1(\mathcal{S},\mathcal{I}_1,\mathcal{I}_2) = \mathcal{S}-\mathcal{S}_1^* &- \int_{\mathcal{S}_1^*}^{\mathcal{S}} \frac{f(\mathcal{S}_1^*,\mathcal{I}_1^*)}{f(X,\mathcal{I}_1^*)}\,dX \\ &+ \mathcal{I}_1^*\left(\frac{\mathcal{I}_1}{\mathcal{I}_1^*}-\ln\frac{\mathcal{I}_1}{\mathcal{I}_1^*}-1\right)+\mathcal{I}_2,\end{aligned}$$

which is non-negative on the interior of $\mathcal{H}$ and vanishes only at $\mathcal{E}_{s_1}$.

Differentiating along the solutions of (5) and using (12), we obtain

$$\begin{aligned}{}^{C}D_t^{\alpha}\mathcal{P}_1 \le{}& \mu\,(\mathcal{S}_1^*-\mathcal{S})\left(1-\frac{f(\mathcal{S}_1^*,\mathcal{I}_1^*)}{f(\mathcal{S},\mathcal{I}_1^*)}\right) \\ &+ (1-u_1)\,\mathcal{I}_1^*\left[\,\xi(\mathcal{S},\mathcal{I}_1)+\Theta(\mathcal{S},\mathcal{I}_1)\,\right] \\ &+ \mathcal{I}_2\left[(1-u_2)\,h(\mathcal{S},\mathcal{I}_2)-(\sigma_2+\mu)\right],\end{aligned} \tag{13}$$

where

$$\xi(\mathcal{S},\mathcal{I}_1) = \frac{f(\mathcal{S}_1^*,\mathcal{I}_1^*)}{f(\mathcal{S},\mathcal{I}_1^*)} - \frac{\mathcal{I}_1}{\mathcal{I}_1^*}$$

and

$$\Theta(\mathcal{S},\mathcal{I}_1) = \frac{f(\mathcal{S},\mathcal{I}_1^*)}{f(\mathcal{S},\mathcal{I}_1)} + \frac{f(\mathcal{S},\mathcal{I}_1)}{f(\mathcal{S},\mathcal{I}_1^*)}\,\frac{\mathcal{I}_1}{\mathcal{I}_1^*} - \frac{\mathcal{I}_1}{\mathcal{I}_1^*} - 1.$$

We estimate the three contributions separately.

First term. By (H_2) the map $X \mapsto f(X, \mathcal{I}_1^*)$ is non-decreasing, so $\mathcal{S}_1^* - \mathcal{S}$ and $1 - f(\mathcal{S}_1^*, \mathcal{I}_1^*)/f(\mathcal{S}, \mathcal{I}_1^*)$ have opposite signs; their product is therefore non-positive.

Second term. The quantity Θ factorizes as

$$\Theta(\mathcal{S}, \mathcal{I}_1) = -\left(1 - \frac{f(\mathcal{S}, \mathcal{I}_1^*)}{f(\mathcal{S}, \mathcal{I}_1)}\right)\left(1 - \frac{f(\mathcal{S}, \mathcal{I}_1)}{f(\mathcal{S}, \mathcal{I}_1^*)}\frac{\mathcal{I}_1}{\mathcal{I}_1^*}\right),$$

and hypothesis (H_3) ensures that the two factors have the same sign, whence $\Theta \leq 0$. As for ξ, hypothesis (H_2) gives $f(\mathcal{S}_1^*, \mathcal{I}_1^*)/f(\mathcal{S}, \mathcal{I}_1^*) \leq 1$ when $\mathcal{S} \geq \mathcal{S}_1^*$, and the reverse inequality otherwise; combined with the first term, the sum remains non-positive.

Third term. On the invariant region $\mathcal{H}$ we have $\mathcal{S} \leq \lambda/\mu$, and (H_2)–(H_3) give $h(\mathcal{S}, \mathcal{I}_2) \leq h(\lambda/\mu, 0)$. Hence

$$\mathcal{I}_2\left[(1-u_2)h(\mathcal{S}, \mathcal{I}_2) - (\sigma_2 + \mu)\right] \leq (\sigma_2 + \mu)\,\mathcal{I}_2\left(R_{0,2} - 1\right) \leq 0$$

whenever $R_{0,2} \leq 1$.

Collecting the three estimates in (13) yields ${}^C D_t^\alpha \mathcal{P}_1 \leq 0$ on $\mathcal{H}$. Equality forces $\mathcal{I}_2 = 0$, $\xi(\mathcal{S}, \mathcal{I}_1) = 0$ and $\Theta(\mathcal{S}, \mathcal{I}_1) = 0$, hence $\mathcal{S} = \mathcal{S}_1^*$ and $\mathcal{I}_1 = \mathcal{I}_1^*$, so that the largest invariant set contained in $\{{}^C D_t^\alpha \mathcal{P}_1 = 0\}$ is the singleton $\{(\mathcal{S}_1^*, \mathcal{I}_1^*, 0)\}$. By the fractional LaSalle invariance principle recalled in Section 2, this equilibrium is globally asymptotically stable for the reduced system, and consequently $\mathcal{E}_{s_1}$ is globally asymptotically stable for (1). □

4.3.3. Global stability of the strain-2 endemic equilibrium

Theorem 7
If $R_{0,1} \leq 1 < R_{0,2}$, then the strain–2 endemic equilibrium $\mathcal{E}_{s_2}$ is globally asymptotically stable.

Proof
Write $\mathcal{E}_{s_2} = (\mathcal{S}_2^*,\, 0,\, \mathcal{I}_2^*,\, \mathcal{R}_2^*)$. This equilibrium satisfies

$$(1-u_2)\,h(\mathcal{S}_2^*, \mathcal{I}_2^*) = \sigma_2 + \mu, \qquad \lambda = \mu\,\mathcal{S}_2^* + (1-u_2)\,h(\mathcal{S}_2^*, \mathcal{I}_2^*)\,\mathcal{I}_2^*, \qquad \mu\,\mathcal{R}_2^* = \sigma_2 \mathcal{I}_2^*. \tag{14}$$

As in the proof of Theorem 6, the equation governing $\mathcal{R}$ is decoupled from the others, so it suffices to establish the result for the reduced system (5).

Consider the Lyapunov functional

$$\mathcal{P}_2(\mathcal{S}, \mathcal{I}_1, \mathcal{I}_2) = \mathcal{S} - \mathcal{S}_2^* - \int_{\mathcal{S}_2^*}^{\mathcal{S}} \frac{h(\mathcal{S}_2^*, \mathcal{I}_2^*)}{h(X, \mathcal{I}_2^*)}\,dX + \mathcal{I}_2^*\left(\frac{\mathcal{I}_2}{\mathcal{I}_2^*} - \ln\frac{\mathcal{I}_2}{\mathcal{I}_2^*} - 1\right) + \mathcal{I}_1,$$

which is non-negative on the interior of $\mathcal{H}$ and vanishes only at $(\mathcal{S}_2^*, 0, \mathcal{I}_2^*)$.

Differentiating along the solutions of (5) and inserting the relations (14), we obtain

$$\begin{aligned} {}^C D_t^\alpha \mathcal{P}_2 \leq\; & \mu\,(\mathcal{S}_2^* - \mathcal{S})\left(1 - \frac{h(\mathcal{S}_2^*, \mathcal{I}_2^*)}{h(\mathcal{S}, \mathcal{I}_2^*)}\right) \\ & + (1-u_2)\,\mathcal{I}_2^*\left[\tilde{\xi}(\mathcal{S}, \mathcal{I}_2) + \tilde{\Theta}(\mathcal{S}, \mathcal{I}_2)\right] \\ & + \mathcal{I}_1\left[(1-u_1)\,f(\mathcal{S}, \mathcal{I}_1) - (\sigma_1 + \mu)\right], \end{aligned} \tag{15}$$

where

$$\tilde{\xi}(\mathcal{S}, \mathcal{I}_2) = \frac{h(\mathcal{S}_2^*, \mathcal{I}_2^*)}{h(\mathcal{S}, \mathcal{I}_2^*)} - \frac{\mathcal{I}_2}{\mathcal{I}_2^*}, \qquad \tilde{\Theta}(\mathcal{S}, \mathcal{I}_2) = \frac{h(\mathcal{S}, \mathcal{I}_2^*)}{h(\mathcal{S}, \mathcal{I}_2)} + \frac{h(\mathcal{S}, \mathcal{I}_2)}{h(\mathcal{S}, \mathcal{I}_2^*)}\frac{\mathcal{I}_2}{\mathcal{I}_2^*} - \frac{\mathcal{I}_2}{\mathcal{I}_2^*} - 1.$$

The three contributions are estimated as follows.

(i) The $\mathcal{S}$-term. By (H_2) the map $X \mapsto h(X, \mathcal{I}_2^*)$ is non-decreasing, so $\mathcal{S}_2^* - \mathcal{S}$ and $1 - h(\mathcal{S}_2^*, \mathcal{I}_2^*)/h(\mathcal{S}, \mathcal{I}_2^*)$ carry opposite signs and their product is non-positive.

(ii) The $\mathcal{I}_2$-block. The quantity $\tilde{\Theta}$ admits the factorization

$$\tilde{\Theta}(\mathcal{S}, \mathcal{I}_2) = -\left(1 - \frac{h(\mathcal{S}, \mathcal{I}_2^*)}{h(\mathcal{S}, \mathcal{I}_2)}\right)\left(1 - \frac{h(\mathcal{S}, \mathcal{I}_2)}{h(\mathcal{S}, \mathcal{I}_2^*)}\frac{\mathcal{I}_2}{\mathcal{I}_2^*}\right),$$

whose two factors have the same sign by (H_3); hence $\tilde{\Theta} \leq 0$. Together with the $\mathcal{S}$-term, the contribution of $\tilde{\xi}$ keeps the sum non-positive.

(iii) The $\mathcal{I}_1$-term. On the invariant region $\mathcal{H}$ one has $\mathcal{S} \leq \lambda/\mu$, and (H_2)–(H_3) give $f(\mathcal{S}, \mathcal{I}_1) \leq f(\lambda/\mu, 0)$. Therefore

$$\mathcal{I}_1\left[(1-u_1)f(\mathcal{S}, \mathcal{I}_1) - (\sigma_1 + \mu)\right] \leq (\sigma_1 + \mu)\,\mathcal{I}_1\left(R_{0,1} - 1\right) \leq 0$$

as soon as $R_{0,1} \leq 1$: the first strain cannot invade and $\mathcal{I}_1$ decays to zero.

Adding the three estimates in (15) gives ${}^{C}D_t^{\alpha}\mathcal{P}_2 \leq 0$ on $\mathcal{H}$. Equality forces $\mathcal{I}_1 = 0$, $\tilde{\xi} = \tilde{\Theta} = 0$, hence $\mathcal{S} = \mathcal{S}_2^*$ and $\mathcal{I}_2 = \mathcal{I}_2^*$; the largest invariant set contained in $\{{}^{C}D_t^{\alpha}\mathcal{P}_2 = 0\}$ is thus the singleton $\{(\mathcal{S}_2^*, 0, \mathcal{I}_2^*)\}$. By the fractional LaSalle invariance principle recalled in Section 2, $\mathcal{E}_{s_2}$ is globally asymptotically stable. □

4.3.4. Global stability of the both endemic equilibrium

Theorem 8
If $R_{0,1} > 1$ and $R_{0,2} > 1$, then the coexisting endemic equilibrium $\mathcal{E}_{s_t}$ is globally asymptotically stable.

Proof

We define the Lyapunov function

$$\begin{aligned}\mathcal{P}_c(\mathcal{S}, \mathcal{I}_1, \mathcal{I}_2, \mathcal{R}) = \mathcal{S} - \mathcal{S}^* - \int_{\mathcal{S}^*}^{\mathcal{S}} \frac{f(\mathcal{S}^*, \mathcal{I}_1^*)\,\mathcal{I}_1^* + h(\mathcal{S}^*, \mathcal{I}_2^*)\,\mathcal{I}_2^*}{f(X, \mathcal{I}_1^*)\,\mathcal{I}_1^* + h(X, \mathcal{I}_2^*)\,\mathcal{I}_2^*}\,dX \\ + \mathcal{I}_1^*\left(\frac{\mathcal{I}_1}{\mathcal{I}_1^*} - \ln\frac{\mathcal{I}_1}{\mathcal{I}_1^*} - 1\right) \\ + \mathcal{I}_2^*\left(\frac{\mathcal{I}_2}{\mathcal{I}_2^*} - \ln\frac{\mathcal{I}_2}{\mathcal{I}_2^*} - 1\right) \\ + \mathcal{R} - \mathcal{R}^* - \mathcal{R}^*\ln\frac{\mathcal{R}}{\mathcal{R}^*}.\end{aligned}$$

The Caputo derivative along the trajectories of the system is

$$\begin{aligned}{}^{C}D_t^{\alpha}\mathcal{P}_c \leq \left(\lambda - f(\mathcal{S}, \mathcal{I}_1)\mathcal{I}_1 - h(\mathcal{S}, \mathcal{I}_2)\mathcal{I}_2 - \mu\,\mathcal{S}\right)\left(1 - \frac{\mathcal{S}^*}{\mathcal{S}}\right) \\ + \left(f(\mathcal{S}, \mathcal{I}_1)\mathcal{I}_1 - (\sigma_1 + \mu)\mathcal{I}_1\right)\left(1 - \frac{\mathcal{I}_1^*}{\mathcal{I}_1}\right) \\ + \left(h(\mathcal{S}, \mathcal{I}_2)\mathcal{I}_2 - (\sigma_2 + \mu)\mathcal{I}_2\right)\left(1 - \frac{\mathcal{I}_2^*}{\mathcal{I}_2}\right) \\ + \left(\sigma_1\mathcal{I}_1 + \sigma_2\mathcal{I}_2 - \mu\,\mathcal{R}\right)\left(1 - \frac{\mathcal{R}^*}{\mathcal{R}}\right).\end{aligned}$$

Substituting the equilibrium relations

$$\begin{cases} \lambda = \mu\,\mathcal{S}^* + f(\mathcal{S}^*,\mathcal{I}_1^*)\mathcal{I}_1^* + h(\mathcal{S}^*,\mathcal{I}_2^*)\mathcal{I}_2^*, \\ f(\mathcal{S}^*,\mathcal{I}_1^*)\mathcal{I}_1^* = (\sigma_1+\mu)\mathcal{I}_1^*, \\ h(\mathcal{S}^*,\mathcal{I}_2^*)\mathcal{I}_2^* = (\sigma_2+\mu)\mathcal{I}_2^*, \\ \sigma_1\mathcal{I}_1^* + \sigma_2\mathcal{I}_2^* = \mu\,\mathcal{R}^*, \end{cases}$$

we analyze each component.

For the $\mathcal{S}$ component we obtain

$$(\lambda - f(\mathcal{S},\mathcal{I}_1)\mathcal{I}_1 - h(\mathcal{S},\mathcal{I}_2)\mathcal{I}_2 - \mu\,\mathcal{S})\left(1 - \frac{\mathcal{S}^*}{\mathcal{S}}\right) \leq 0.$$

For the $\mathcal{I}_1$ component $\quad (f(\mathcal{S},\mathcal{I}_1)\mathcal{I}_1 - (\sigma_1+\mu)\mathcal{I}_1)\left(1 - \frac{\mathcal{I}_1^*}{\mathcal{I}_1}\right) = -\frac{(\sigma_1+\mu)(\mathcal{I}_1-\mathcal{I}_1^*)^2}{\mathcal{I}_1} \leq 0.$

For the $\mathcal{I}_2$ component $\quad (h(\mathcal{S},\mathcal{I}_2)\mathcal{I}_2 - (\sigma_2+\mu)\mathcal{I}_2)\left(1 - \frac{\mathcal{I}_2^*}{\mathcal{I}_2}\right) = -\frac{(\sigma_2+\mu)(\mathcal{I}_2-\mathcal{I}_2^*)^2}{\mathcal{I}_2} \leq 0.$

For the $\mathcal{R}$ component $\quad (\sigma_1\mathcal{I}_1 + \sigma_2\mathcal{I}_2 - \mu\,\mathcal{R})\left(1 - \frac{\mathcal{R}^*}{\mathcal{R}}\right) = -\mu\,\frac{(\mathcal{R}-\mathcal{R}^*)^2}{\mathcal{R}} \leq 0.$

Thus $\quad {}^{C}D_t^{\alpha}\mathcal{P}_c \leq 0$

with equality only at $\quad (\mathcal{S},\mathcal{I}_1,\mathcal{I}_2,\mathcal{R}) = (\mathcal{S}^*,\mathcal{I}_1^*,\mathcal{I}_2^*,\mathcal{R}^*).$

Therefore, by LaSalle's invariance principle for fractional-order systems, all trajectories converge to the endemic equilibrium $\mathcal{E}_{s_t}$.

Hence the coexistence equilibrium is globally asymptotically stable whenever $R_{0,1} > 1$ and $R_{0,2} > 1$.

□

5. Optimal control study

In this section we introduce two time-dependent treatment controls $u_1(t)$ and $u_2(t)$ and look for an optimal pair (u_1^*, u_2^*) that reduces the number of infected individuals at the lowest possible intervention cost.

5.1. The controlled model

The controlled fractional $\mathcal{S}\mathcal{I}_1\mathcal{I}_2\mathcal{R}$ model reads

$$\begin{cases} {}^{C}D_t^{\alpha}\mathcal{S}(t) = \lambda - (1-u_1(t))\,f(\mathcal{S},\mathcal{I}_1)\,\mathcal{I}_1 - (1-u_2(t))\,h(\mathcal{S},\mathcal{I}_2)\,\mathcal{I}_2 - \mu\,\mathcal{S}, \\ {}^{C}D_t^{\alpha}\mathcal{I}_1(t) = (1-u_1(t))\,f(\mathcal{S},\mathcal{I}_1)\,\mathcal{I}_1 - (\sigma_1+\mu)\,\mathcal{I}_1, \\ {}^{C}D_t^{\alpha}\mathcal{I}_2(t) = (1-u_2(t))\,h(\mathcal{S},\mathcal{I}_2)\,\mathcal{I}_2 - (\sigma_2+\mu)\,\mathcal{I}_2, \\ {}^{C}D_t^{\alpha}\mathcal{R}(t) = \sigma_1\mathcal{I}_1 + \sigma_2\mathcal{I}_2 - \mu\,\mathcal{R}, \end{cases} \tag{16}$$

with the same non-negative initial data as in (1). Biologically, $u_i(t)$ is the fraction of new infections of strain i prevented by treatment at time t: the value $u_i = 0$ corresponds to no intervention and $u_i = 1$ to a complete interruption of transmission.

5.2. The optimal control problem

Over a fixed therapeutic horizon $[0, t_e]$, we consider the cost functional

$$J(u_1,u_2) = \int_0^{t_e} \left(A_1\,\mathcal{I}_1(t) + A_2\,\mathcal{I}_2(t) + \frac{C_1}{2}\,u_1^2(t) + \frac{C_2}{2}\,u_2^2(t)\right) dt, \tag{17}$$

where A_1 and A_2 are positive weights measuring the relative burden of each strain, and where the positive constants C_1 and C_2 represent the unit costs of the two treatment strategies. The quadratic form of the control terms reflects the fact that the marginal cost of an intervention increases with its intensity.

The admissible control set is

$$U = \{(u_1, u_2) \ : \ u_i \text{ Lebesgue measurable}, \ 0 \leq u_i(t) \leq 1 \text{ for a.e. } t \in [0, t_e], \ i = 1, 2\}, \tag{18}$$

and the problem consists in finding $(u_1^*, u_2^*) \in U$ such that

$$J(u_1^*, u_2^*) = \min_{(u_1,u_2)\in U} J(u_1, u_2). \tag{19}$$

5.3. Existence and uniqueness of the state solution

Theorem 9
For every admissible pair $(u_1, u_2) \in U$, system (16) admits a unique non-negative solution defined on $[0, t_e]$ and remaining in the region $\mathcal{H}$.

Proof
Since $0 \leq u_i \leq 1$, the right-hand side of (16) differs from that of (1) only by the bounded factors $(1 - u_i)$. The arguments used in the proof of Proposition 1 therefore apply verbatim: the vector field is locally Lipschitz on $\mathbb{R}^4_+$ by (H_1), it points inwards on the faces of the positive orthant, and the total population still satisfies ${}^C D_t^\alpha \mathcal{N} = \lambda - \mu\mathcal{N}$, so that $\mathcal{H}$ remains positively invariant. Existence, uniqueness and boundedness follow. □

5.4. Existence of an optimal control

Theorem 10
There exists an optimal pair $(u_1^*, u_2^*) \in U$ solving (19).

Proof
We verify the conditions of the classical existence theorem for optimal control problems (see Ref. [19]).

1. The set of admissible controls together with the associated state trajectories is non-empty, since $u_1 = u_2 = 0$ is admissible and Theorem 9 provides the corresponding solution.
2. U is convex and closed by definition (18).
3. The right-hand side of (16) is bounded by a linear function of the state, because the trajectories remain in the compact set $\mathcal{H}$ and the controls take values in $[0, 1]$.
4. The integrand of (17) is convex on U, being the sum of a term independent of the controls and of the strictly convex quadratic form $\frac{C_1}{2}u_1^2 + \frac{C_2}{2}u_2^2$.
5. There exist constants $c_1 > 0$, $c_2 > 0$ and $\rho > 1$ such that the integrand is bounded below by $c_1 \left(|u_1|^2 + |u_2|^2\right)^{\rho/2} - c_2$; it suffices to take $\rho = 2$, $c_1 = \min\{C_1, C_2\}/2$ and $c_2 = 0$.

The conclusion follows. □

5.5. Pontryagin's Maximum Principle

In order to characterize the optimal controls, we form the Hamiltonian associated with problem (19),

$$\begin{aligned} H = {} & A_1\mathcal{I}_1 + A_2\mathcal{I}_2 + \frac{C_1}{2}u_1^2 + \frac{C_2}{2}u_2^2 \\ & + \lambda_1\Big[\lambda - (1-u_1)f(\mathcal{S},\mathcal{I}_1)\mathcal{I}_1 - (1-u_2)h(\mathcal{S},\mathcal{I}_2)\mathcal{I}_2 - \mu\mathcal{S}\Big] \\ & + \lambda_2\Big[(1-u_1)f(\mathcal{S},\mathcal{I}_1)\mathcal{I}_1 - (\sigma_1+\mu)\mathcal{I}_1\Big] \\ & + \lambda_3\Big[(1-u_2)h(\mathcal{S},\mathcal{I}_2)\mathcal{I}_2 - (\sigma_2+\mu)\mathcal{I}_2\Big] \\ & + \lambda_4\Big[\sigma_1\mathcal{I}_1 + \sigma_2\mathcal{I}_2 - \mu\mathcal{R}\Big], \end{aligned} \tag{20}$$

where $\lambda_1, \ldots, \lambda_4$ are the adjoint variables.

Theorem 11
Let (u_1^*, u_2^*) be an optimal pair and let $(\mathcal{S}^*, \mathcal{I}_1^*, \mathcal{I}_2^*, \mathcal{R}^*)$ be the associated state trajectory. Then there exist adjoint functions $\lambda_1, \ldots, \lambda_4$ satisfying the backward system

$$\begin{cases} {}_tD_{t_e}^{\alpha}\lambda_1 = \mu\lambda_1 + (\lambda_1 - \lambda_2)(1-u_1^*)\dfrac{\partial f}{\partial \mathcal{S}}\mathcal{I}_1 + (\lambda_1 - \lambda_3)(1-u_2^*)\dfrac{\partial h}{\partial \mathcal{S}}\mathcal{I}_2, \\ {}_tD_{t_e}^{\alpha}\lambda_2 = -A_1 + (\lambda_1 - \lambda_2)(1-u_1^*)\left(f + \mathcal{I}_1\dfrac{\partial f}{\partial \mathcal{I}_1}\right) + (\sigma_1 + \mu)\lambda_2 - \sigma_1\lambda_4, \\ {}_tD_{t_e}^{\alpha}\lambda_3 = -A_2 + (\lambda_1 - \lambda_3)(1-u_2^*)\left(h + \mathcal{I}_2\dfrac{\partial h}{\partial \mathcal{I}_2}\right) + (\sigma_2 + \mu)\lambda_3 - \sigma_2\lambda_4, \\ {}_tD_{t_e}^{\alpha}\lambda_4 = \mu\lambda_4, \end{cases} \tag{21}$$

where ${}_tD_{t_e}^{\alpha}$ denotes the right Riemann–Liouville fractional derivative, together with the transversality conditions

$$\lambda_i(t_e) = 0, \qquad i = 1, \ldots, 4.$$

Moreover, the optimal controls are characterized by

$$\begin{aligned} u_1^*(t) &= \min\left\{1,\ \max\left\{0,\ \frac{(\lambda_2 - \lambda_1)\, f(\mathcal{S}, \mathcal{I}_1)\, \mathcal{I}_1}{C_1}\right\}\right\}, \\ u_2^*(t) &= \min\left\{1,\ \max\left\{0,\ \frac{(\lambda_3 - \lambda_1)\, h(\mathcal{S}, \mathcal{I}_2)\, \mathcal{I}_2}{C_2}\right\}\right\}. \end{aligned} \tag{22}$$

Proof
The adjoint system (21) is obtained from

$${}_tD_{t_e}^{\alpha}\lambda_1 = -\frac{\partial H}{\partial \mathcal{S}}, \quad {}_tD_{t_e}^{\alpha}\lambda_2 = -\frac{\partial H}{\partial \mathcal{I}_1}, \quad {}_tD_{t_e}^{\alpha}\lambda_3 = -\frac{\partial H}{\partial \mathcal{I}_2}, \quad {}_tD_{t_e}^{\alpha}\lambda_4 = -\frac{\partial H}{\partial \mathcal{R}},$$

the transversality conditions expressing that the terminal state is free. Since H is strictly convex in (u_1, u_2), the optimality conditions $\dfrac{\partial H}{\partial u_i} = 0$ on the interior of U give

$$C_1 u_1 + (\lambda_1 - \lambda_2) f(\mathcal{S}, \mathcal{I}_1)\mathcal{I}_1 = 0, \qquad C_2 u_2 + (\lambda_1 - \lambda_3) h(\mathcal{S}, \mathcal{I}_2)\mathcal{I}_2 = 0,$$

hence $u_1 = \dfrac{(\lambda_2 - \lambda_1) f(\mathcal{S}, \mathcal{I}_1)\mathcal{I}_1}{C_1}$ and $u_2 = \dfrac{(\lambda_3 - \lambda_1) h(\mathcal{S}, \mathcal{I}_2)\mathcal{I}_2}{C_2}$. Projecting these expressions onto $[0, 1]$ yields (22). □

The state system (16), the adjoint system (21) and the characterization (22) form the optimality system, which is solved numerically in Section 6 by a forward–backward sweep method: the state equations are integrated forward in time, the adjoint equations backward, and the controls are updated at each iteration until convergence.

6. Numerical simulations and discussions

In this section, we present some numerical simulations to illustrate the effects of the fractional derivative and treatment parameters on the spread of infection. These simulations were performed using MATLAB. The first numerical simulation was carried out using the fractional Adams–Bashforth–Moulton predictor–corrector scheme

presented in [3]. More precisely, the numerical discretization is given by::

$$U(t_j) = \frac{h^\alpha}{\Gamma(\alpha+2)}\Big((j-1)^{\alpha+1} - (j-\alpha-1)j^\alpha\Big)\mathcal{F}(U(t_0)) + U(t_0)$$
$$+ \frac{h^\alpha}{\Gamma(\alpha+2)}\sum_{i=1}^{j-1}\Big((j-i+1)^{\alpha+1} - 2(j-i)^{\alpha+1} + (j-i-1)^{\alpha+1}\Big)\mathcal{F}(U(t_i))$$
$$+ \frac{h^\alpha}{\Gamma(\alpha+2)}\mathcal{F}(U(t_{j-1})) + \frac{h^\alpha}{\Gamma(\alpha+1)}\mathcal{F}(U(t_{j-1})),$$

where $t_j = t_0 + (j-1)h$, for $j = 0, 1, \ldots, N-1$.

6.1. Numerical convergence and role of the fractional order

The purpose of this subsection is twofold: to verify numerically the stability results established in Section 4.3, and to clarify what the Caputo order α actually adds to the description of the epidemic. The initial state is $\big(\mathcal{S}(0), \mathcal{I}_1(0), \mathcal{I}_2(0), \mathcal{R}(0)\big) = (0.5,\ 0.8,\ 0.8,\ 0.2)$, and four orders are compared, $\alpha \in \{1,\ 0.9,\ 0.7,\ 0.5\}$. The incidence functions are specialised as

$$f(\mathcal{S}, \mathcal{I}_1) = \frac{\beta_1 \mathcal{S}}{1 + m\,\mathcal{I}_1^2}, \qquad h(\mathcal{S}, \mathcal{I}_2) = \beta_2 \mathcal{S},$$

the first one being non-monotone in $\mathcal{I}_1$ (psychological or behavioural saturation effect), the second one bilinear. Both satisfy hypotheses (H_1)–(H_3). The parameter values are $\lambda = 1$, $\beta_1 = 0.06$, $\beta_2 = 0.6$, $\sigma_1 = 0.15$, $\sigma_2 = 0.25$, $\mu = 0.2$, $m = 0.14$, and no control is applied. With these data one obtains $R_{0,1} = 0.8571$ and $R_{0,2} = 6.6667$. Only the second threshold exceeds unity, so Theorem 8 applies and the strain-1 free endemic equilibrium $\mathcal{E}_2 = \big(\mathcal{S}^*,\ \mathcal{I}_1^*,\ \mathcal{I}_2^*,\ \mathcal{R}^*\big) = (0.7500,\ 0,\ 1.8889,\ 2.3611)$ is the attractor of the system. Figure 3 agrees with this prediction for every order tested: $\mathcal{I}_1$ decays monotonically to zero while $\mathcal{I}_2$ settles on its endemic level, and the total population tends to $\dfrac{\lambda}{\mu} = 5$. Competitive exclusion occurs here because the saturation term $1 + m\mathcal{I}_1^2$ weakens the first strain as soon as it starts to spread, whereas the bilinear incidence of the second strain suffers no such penalty. A point worth emphasising is that the four curves of a given compartment share the same limit. Neither the thresholds $R_{0,i}$ nor the coordinates of $\mathcal{E}_2$ involve α; the fractional order acts on the way the trajectory reaches its limit, not on the limit itself.

Biological effect of α In the integer-order setting ($\alpha = 1$) the state of the epidemic at time t determines its instantaneous variation, and nothing else. Replacing the ordinary derivative by the Caputo operator introduces the kernel $(t-s)^{-\alpha}/\Gamma(1-\alpha)$, which weights every past instant $s < t$ with a slowly decaying factor. The order α then measures how heavily the history of the outbreak still bears on its present evolution.

Three epidemiological mechanisms are captured this way. First, residual immunity and partial cross-protection between the two strains: an individual who has been exposed earlier does not respond to a new contact as a naive individual would, and the exponentially distributed sojourn times implicitly assumed by classical ODE models are known to be a poor description of latent and infectious periods. Second, the inertia of collective behaviour: risk perception, mask wearing or treatment adherence build up as the epidemic unfolds and fade away only gradually once it recedes, so the effective contact rate lags behind the reported incidence. Third, the sub-diffusive character of propagation on heterogeneous contact networks, where clustered mobility produces a slower-than-exponential spread. Values of α close to 1 correspond to a population that reacts instantaneously and forgets quickly; small values describe a population whose past strongly conditions its present.

The simulations make this distinction concrete. Lowering α flattens the curve of $\mathcal{I}_2$, reduces and postpones its maximum, and stretches the transient phase well beyond what the classical model predicts; the plateau $\mathcal{I}_2^* = 1.8889$ is nevertheless reached in every case. In practical terms, a population with pronounced memory faces a milder epidemic wave, which eases the instantaneous burden on hospital capacity, but that wave lasts longer and control measures must be sustained accordingly. Since the two effects work in opposite directions, the choice of α is not

a mere fitting device: it changes the timing on which an intervention should be planned, which is precisely what motivates the optimal control problem addressed in Section 5. The sensitivity indices reported in Table 3 complete this picture by quantifying the influence of the remaining parameters on the two thresholds.

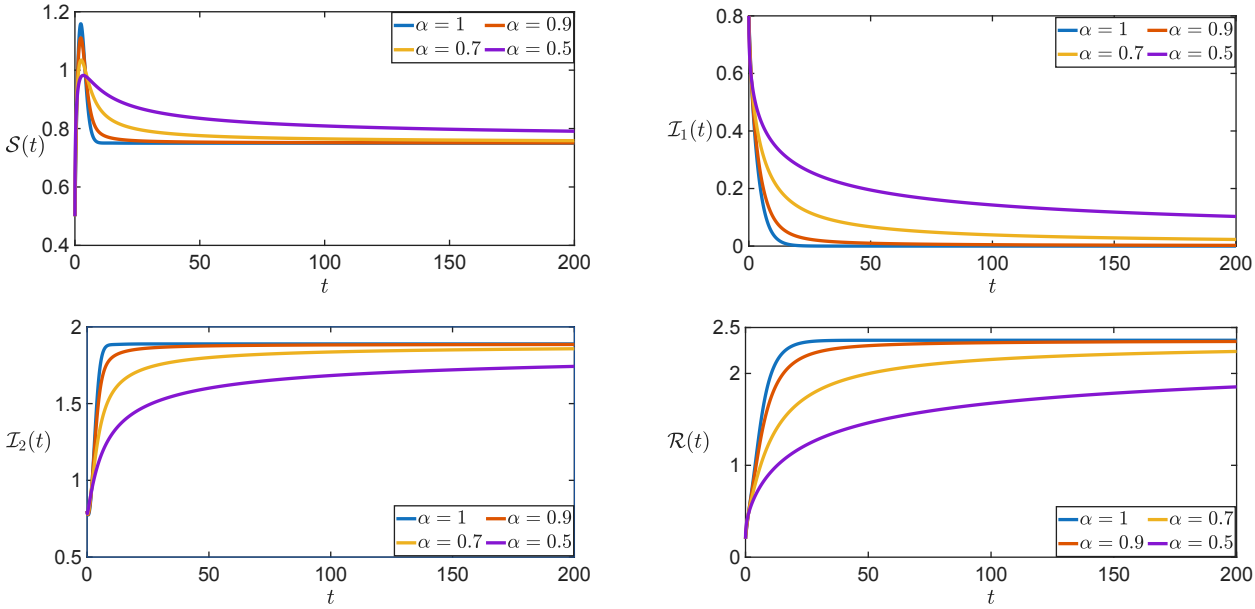

Figure 3. Evolution of $\mathcal{S}(t), \mathcal{I}_1(t), \mathcal{I}_2(t)$ and $\mathcal{R}(t)$ for $\alpha \in \{1,\ 0.9,\ 0.7,\ 0.5\}$. The first strain vanishes, the second one persists, and all trajectories converge to $\mathcal{E}_2$. Decreasing the fractional order slows down the approach to the equilibrium without altering it.

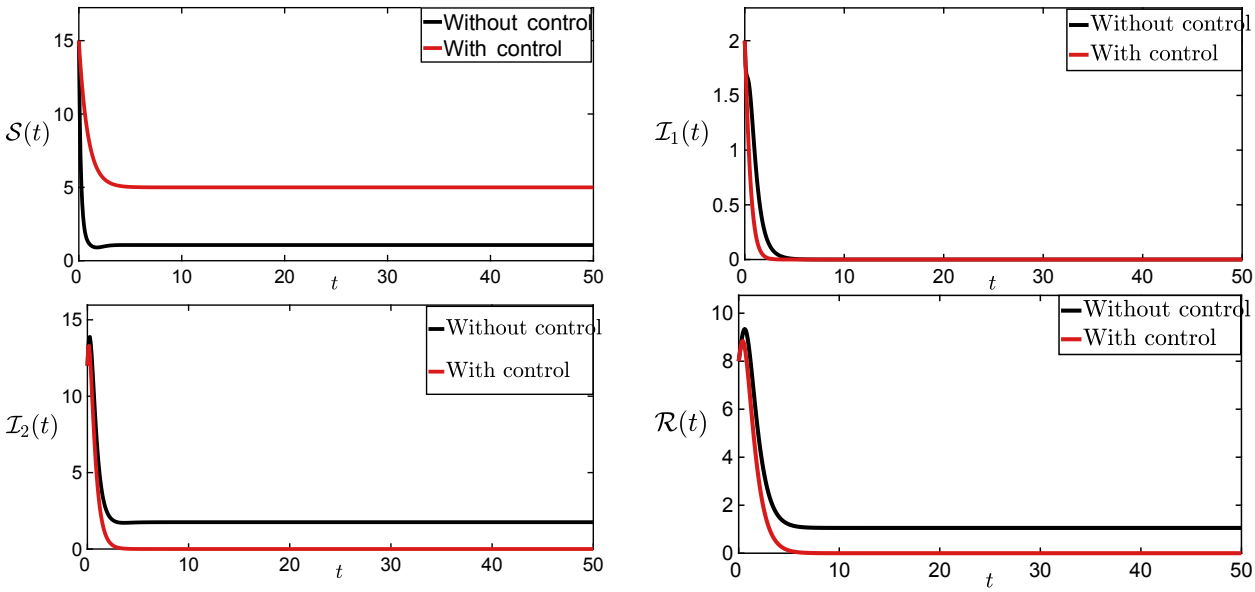

Figure 4. Dynamics of the $\mathcal{SIR}$ model with non-monotone incidence for $\alpha = 0.5$: comparison of the four compartments without control (black) and with optimal control (red).

6.2. *Effect of the optimal control strategy*

The stability behavior of the coexistence endemic equilibrium $\mathcal{E}_{s_t}$ is investigated under non-monotonic incidence functions $f(\mathcal{S},\mathcal{I}_1) = \dfrac{\beta_1 \mathcal{S}}{1+m\mathcal{I}^2}$ and $h(\mathcal{S},\mathcal{I}_2) = \beta_2 \mathcal{S}\mathcal{I}_2$. The parameter set is taken from [23]: $\lambda = 1$, $\beta_1 = \beta_2 = 0.6$, $\alpha_1 = \alpha_2 = 0.5$, $\sigma_1 = \sigma_2 = 0.15$, $\mu = 0.2$, $m = 0.14$. Under these conditions, the system converges towards the steady state $(0.8982, 0.5904, 0.5815, 0.8433, 0.8309, 1.2557)$ with $R_{0,1} = R_{0,2} = 6.1224$, confirming $R_{0,1} > 1$ and $R_{0,2} > 1$ and the global asymptotic stability of the coexistence equilibrium $\mathcal{E}_{s_t}$.

Figure 4 corresponds to the strongest memory considered here, $\alpha = 0.5$. In the absence of treatment (black curves), both infected compartments rise quickly and then settle on a plateau that they leave only very slowly: the power-law kernel keeps the early stages of the outbreak influencing the incidence long after the initial peak, so the susceptible pool is never given the time to recover. Switching on the two controls (red curves) changes the picture within the first weeks of therapy. Both $\mathcal{I}_1$ and $\mathcal{I}_2$ are pushed down well below their uncontrolled level, $\mathcal{S}$ climbs back towards its disease-free value, and $\mathcal{R}$ grows faster because recoveries are no longer offset by a continuous stream of new infections. Two features are worth pointing out. First, the reduction is not uniform in time: the controls act most strongly around the epidemic peak, which is precisely where the adjoint variables $\lambda_2 - \lambda_1$ and $\lambda_3 - \lambda_1$ in (22) are largest. Second, the gap between the two curves does not close at the end of the horizon, indicating that the benefit of the intervention persists beyond the treatment window itself — an effect that an integer-order model cannot reproduce.

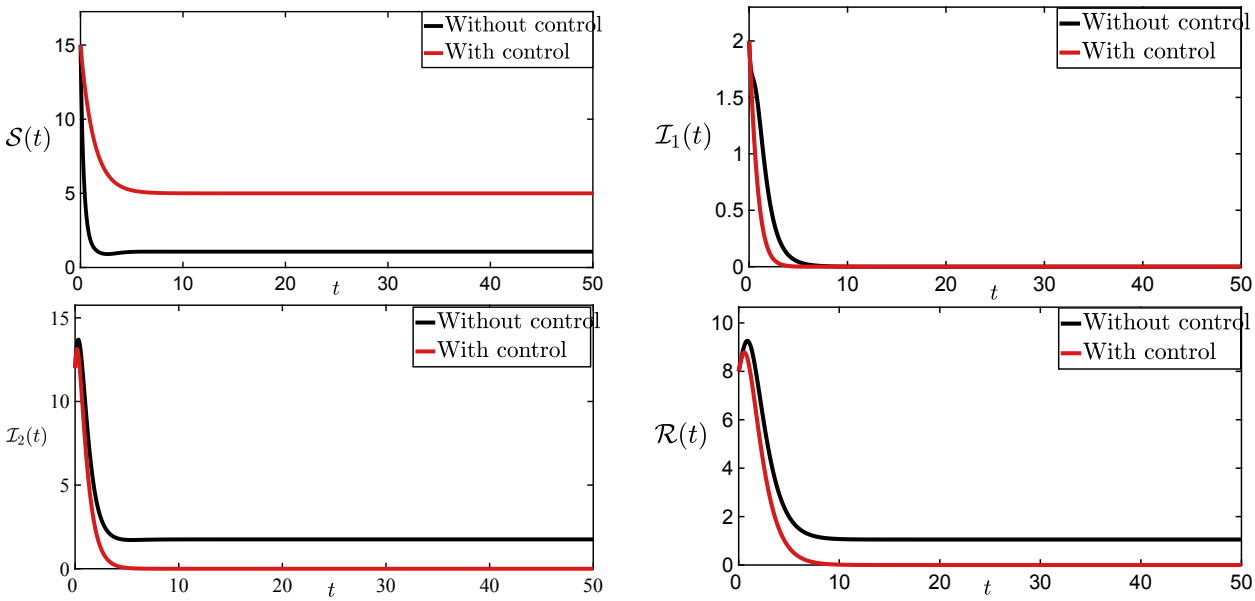

Figure 5. Dynamics of the four compartments for $\alpha = 0.7$: without control (black) and under the optimal strategy (u_1^*, u_2^*) (red).

Raising the order to $\alpha = 0.7$ (Figure 5) shortens the transient phase without altering its qualitative shape. The uncontrolled epidemic now reaches its maximum earlier and the approach to the endemic level is visibly faster, which is consistent with the weaker weight given to the past by the kernel $(t-s)^{-\alpha}/\Gamma(1-\alpha)$ as α increases. The controlled trajectories follow the same trend: the peaks of $\mathcal{I}_1$ and $\mathcal{I}_2$ are again substantially lowered, but the two curves — controlled and uncontrolled — separate sooner than for $\alpha = 0.5$, since the system reacts more promptly to the treatment. In other words, less memory means a shorter epidemic but also a narrower window during which the intervention has to be applied to be effective.

For $\alpha = 0.9$ (Figure 6) the trajectories already resemble those of the classical model, yet the residual memory remains perceptible in the tail of the curves, where the convergence towards the steady state is still slower than

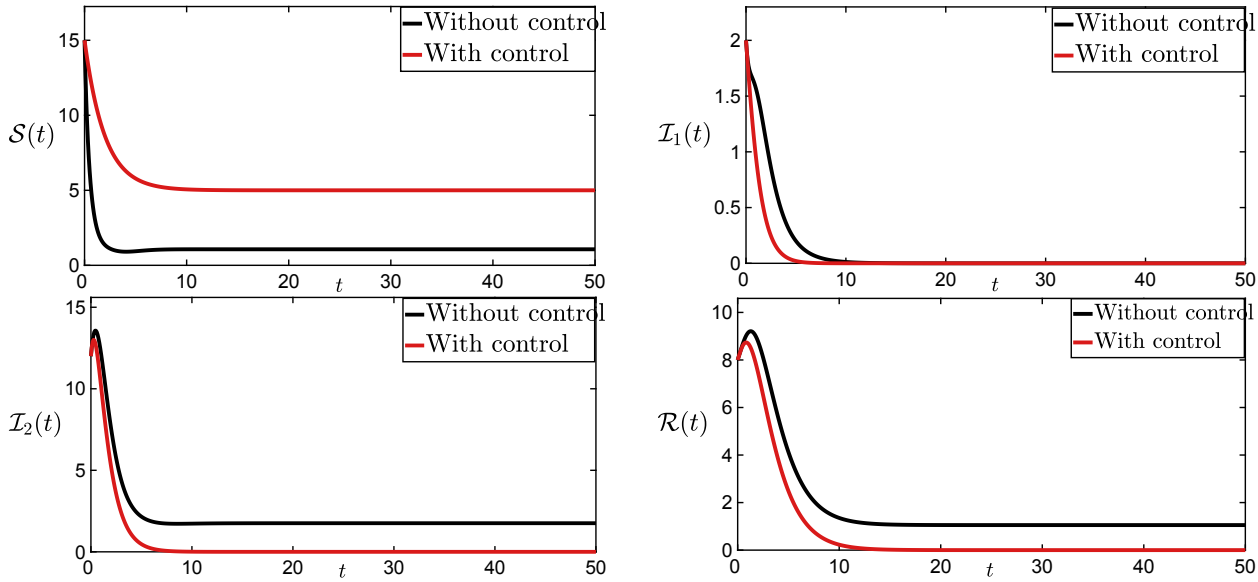

Figure 6. Dynamics of the four compartments for $\alpha = 0.9$: without control (black) and under the optimal strategy (u_1^*, u_2^*) (red).

exponential. The controls act more sharply than in the previous cases: the peak of $\mathcal{I}_2$ is cut earlier and the corresponding rise of $\mathcal{S}$ is steeper. This is a direct consequence of the state equations: with little memory, a reduction in the incidence at time t translates almost immediately into a reduction of the infected populations, whereas for small α part of the effort is spent compensating the transmissions that occurred earlier.

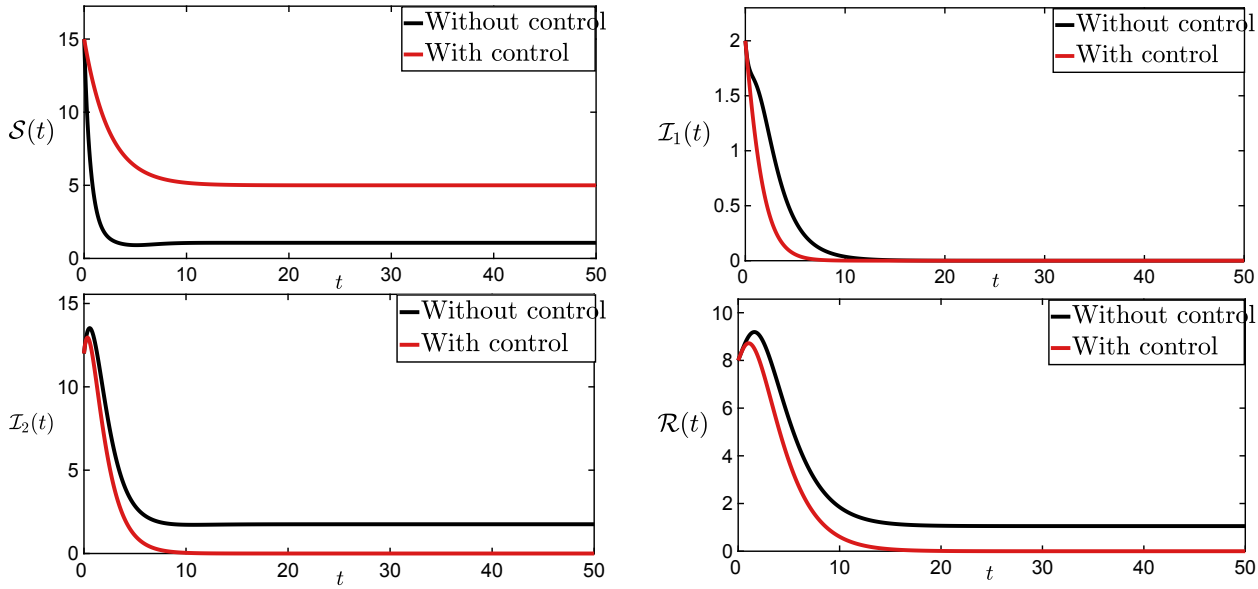

Figure 7. Dynamics of the four compartments for $\alpha = 1$: without control (black) and under the optimal strategy (u_1^*, u_2^*) (red).

The integer-order case $\alpha = 1$ (Figure 7) serves as a reference. Without treatment the outbreak is the fastest and the sharpest of the four scenarios: the infected compartments peak early and the susceptible population drops abruptly before stabilising. Under the optimal strategy the peaks are markedly reduced and $\mathcal{S}$ is maintained at a higher level throughout the horizon. Comparing this figure with Figures 4–6 makes the role of α explicit: the classical model overestimates both the height of the peak and the speed at which the epidemic resolves, and it consequently underestimates the duration over which control measures must be sustained. Taken together, the four scenarios $\alpha = 1,\ 0.9,\ 0.7,\ 0.5$ deliver a consistent message. Decreasing the fractional order slows down the convergence of $\mathcal{I}_1$ and $\mathcal{I}_2$ towards their endemic values and flattens the epidemic curve, while the asymptotic levels of $\mathcal{S}$ and $\mathcal{R}$ are essentially unchanged — as expected, since the equilibria computed in Section 4 do not depend on α. From a public-health standpoint this distinction matters: a population with pronounced memory faces a milder but longer epidemic wave, so that the pressure on healthcare capacity is lower at any given moment but extends over a longer period. The optimal controls remain effective across the whole range of orders tested, which indicates that the strategy derived in Section 5 is robust with respect to the amount of memory assumed. What changes with α is not whether the intervention works, but when it should be deployed and for how long.

7. Conclusion

In this paper, we investigated the dynamics of a fractional-order two-strain $\mathcal{SI}_1\mathcal{I}_2\mathcal{R}$ epidemic model incorporating general nonlinear incidence functions and optimal control strategies. We established the well-posedness of the model by proving the existence, positivity and boundedness of solutions. The disease-free and endemic equilibria associated with each strain, as well as the coexistence equilibrium, were determined and their stability properties analyzed by means of the basic reproduction numbers and of suitable Lyapunov functionals. An optimal control problem was then formulated in order to minimize the number of infected individuals while keeping the intervention costs under control. Applying Pontryagin's Maximum Principle, we derived the necessary optimality conditions and characterized the optimal treatment strategies.

The numerical study clarifies the role played by the fractional order. The thresholds $R_{0,1}$ and $R_{0,2}$, and hence the equilibrium eventually reached by the system, do not involve α: what the order governs is the way that limit is approached. Decreasing α strengthens the weight given to the history of the outbreak, which flattens the epidemic curve, delays and lowers its peak, and lengthens the transient phase well beyond what the classical model predicts. A population with pronounced memory therefore experiences a milder but more protracted wave, so that the instantaneous pressure on healthcare capacity is reduced while the period during which measures must be maintained is extended. Neglecting this effect, as an integer-order formulation implicitly does, leads to overestimating the height of the peak and underestimating the duration of the intervention. The sensitivity analysis complements this picture by ranking the remaining parameters: the transmission rates β_i and the recruitment rate λ act positively on the reproduction numbers with unit elasticity, whereas the recovery rates and the controls act in the opposite direction. Since the mortality rate cannot be used as a lever, the transmission rates remain the most efficient target for an intervention aiming at bringing $R_{0,i}$ below unity. Regarding the effect of the controls, the simulations show a substantial reduction of the infection peaks, higher susceptible levels throughout the therapeutic horizon and a faster growth of the recovered class. This holds for every order tested, which suggests that the strategy derived here is robust with respect to the amount of memory assumed; what changes with α is the timing of the effort rather than its efficacy. A further consequence of leaving the two incidence functions unspecified deserves to be emphasised. Because f and h may respond differently to the depletion of susceptibles, the model produces competitive exclusion in situations where both reproduction numbers exceed unity — a behaviour that cannot be observed when the two strains are assigned the same functional form of incidence. The saturation term of the non-monotone incidence penalises the corresponding strain as soon as it spreads, and this alone can decide the outcome of the competition, even for identical transmission and recovery rates. Several directions remain open. The model is formulated in general terms and has not been calibrated against epidemiological data; confronting it with incidence records for a disease presenting two competing variants would allow the fractional order to be estimated rather than prescribed, and would turn the qualitative conclusions drawn here into quantitative predictions. Introducing

vaccination as a third control, allowing cross-immunity between the two strains, or replacing the deterministic setting by a stochastic one are natural extensions. Spatial heterogeneity, through a reaction–diffusion formulation, would be another relevant development.

Acknowledgement

The authors gratefully acknowledge the editor and the reviewers for their valuable remarks and suggestions, which have significantly improved the quality of the manuscript.

REFERENCES

1. H. Aghdaoui, A. Lamrani Alaoui, K.S. Nisar, M. Tilioua. On Analysis and Optimal Control of a SEIRI Epidemic Model with General Incidence Rate. *Results Phys.*, 20, 103681 (2021). https://doi.org/10.1016/j.rinp.2020.103681
2. C. Alfiniyah, F.P. Batubara, A. Ahmadin, R. Gweryina. Modeling and optimal control analysis of Lassa fever with lockdown and treatment interventions. *Stat. Optim. Inf. Comput.*, 16(2), 1243–1254 (2026).
3. K. Akdim, A. Ez-Zetouni, M. Zahid. The influence of awareness campaigns on the spread of an infectious disease: a qualitative analysis of a fractional epidemic model. *Model. Earth Syst. Environ.*, 8(1), 1311–1319 (2022). https://doi.org/10.1007/s40808-021-01158-9
4. K. Allali, J. Danane, Y. Kuang. Global analysis for an HIV infection model with CTL immune response and infected cells in eclipse phase. *Appl. Sci.*, 7(8), 861 (2017). https://doi.org/10.3390/app7080861
5. K. Allali, S. Harroudi, D.F.M. Torres. Analysis and optimal control of an intracellular delayed HIV model with CTL immune response. *Math. Comput. Sci.*, 12(2), 111–127 (2018). https://doi.org/10.1007/s11786-018-0333-9
6. K. Allali, S. Harroudi, D.F.M. Torres. Optimal control of an HIV model with a trilinear antibody growth function. *Discrete Contin. Dyn. Syst. Ser. S*, 15(3), 501–518 (2022). https://doi.org/10.3934/dcdss.2021148
7. K. Allali, Y. Tabit, S. Harroudi. On HIV model with adaptive immune response, two saturated rates and therapy. *Math. Model. Nat. Phenom.*, 12(5), 1–14 (2017).
8. I.A. Baba, E. Hincal. Global stability analysis of two-strain epidemic model with bilinear and nonmonotone incidence rates. *Eur. Phys. J. Plus*, 132(5), 208 (2017). https://doi.org/10.1140/epjp/i2017-11476-x
9. L.D.R. Beal, D. Hill, R.A. Martin, J. Hedengren. GEKKO Optimization Suite. *Processes*, 6(8), 106 (2018). https://doi.org/10.3390/pr6080106
10. J.W. Bebernes. The stability of dynamical systems (J.P. LaSalle). *SIAM Rev.*, 21(3), 418–420 (1979). https://doi.org/10.1137/1021079
11. D. Bentaleb, S. Harroudi, S. Amine, K. Allali. Analysis and optimal control of a multistrain SEIR epidemic model with saturated incidence rate and treatment. *Differ. Equ. Dyn. Syst.*, 31(4), 907–923 (2023). https://doi.org/10.1007/s12591-020-00544-6
12. A. Boukhouima, E.M. Lotfi, M. Mahrouf, N. Yousfi, T. Kuniya. A general fractional-order viral infection model with cell-to-cell transmission and adaptive immunity. *Prog. Fract. Differ. Appl.*, 9(1), 41–63 (2023). https://doi.org/10.18576/pfda/090103
13. C. Bounkaicha, K. Allali. A fractional derivative perspective on modeling the dynamics of hepatitis C virus with spatial diffusion and CTL immune response. *Int. J. Dyn. Control*, 13(10), 353 (2025).
14. J. Danane, K. Allali, Z. Hammouch. Mathematical analysis of a fractional differential model of HBV infection with antibody immune response. *Chaos Solitons Fractals*, 136, 109787 (2020). https://doi.org/10.1016/j.chaos.2020.109787
15. J. Danane, Z. Hammouch, K. Allali, S. Rashid, J. Singh. A fractional-order model of coronavirus disease 2019 (COVID-19) with governmental action and individual reaction. *Math. Methods Appl. Sci.*, 46(7), 8275–8288 (2023). https://doi.org/10.1002/mma.7759
16. M. Elkaf, A. Meskaf, K. Allali. Mathematical Modeling of HBV Infection with DNA-Containing Capsids and Therapy. In *Nonlinear Dynamics and Complexity: Mathematical Modelling of Real-World Problems*, Springer, 2022. https://doi.org/10.1007/978-3-031-06632-0
17. M. El-Shahed, A. Alsaedi. On the fractional-order SEIR epidemic model with nonlinear incidence rate. *Appl. Math. Lett.*, 24(7), 1179–1184 (2011). https://doi.org/10.1016/j.aml.2011.01.034
18. F.E. Fikri, K. Allali. HIV Dynamics with a Trilinear Antibody Growth Function and Saturated Infection Rate. *Math. Comput. Appl.*, 27(5), 85 (2022). https://doi.org/10.3390/mca27050085
19. W. Fleming, R. Rishel. *Deterministic and Stochastic Optimal Control*. Springer, New York, 1975.
20. J.A. Gallegos, M.A. Duarte-Mermoud. On the Lyapunov theory for fractional order systems. *Appl. Math. Comput.*, 287–288, 161–170 (2016). https://doi.org/10.1016/j.amc.2016.04.039
21. S. Harroudi, D. Bentaleb, Y. Tabit, S. Amine, K. Allali. Optimal control of an HIV infection model with the adaptive immune response and two saturated rates. *Int. J. Math. Comput. Sci.*, 14, 787–807 (2019).
22. W.O. Kermack, A.G. McKendrick. A Contribution to the Mathematical Theory of Epidemics. *Proc. R. Soc. Lond. A*, 115, 700–721 (1927). https://doi.org/10.1098/rspa.1927.0118
23. O. Khyar, K. Allali. Global dynamics of a multi-strain SEIR epidemic model with general incidence rates: application to COVID-19 pandemic. *Nonlinear Dyn.*, 102, 489–509 (2020). https://doi.org/10.1007/s11071-020-05929-4

24. O. Khyar, A. Meskaf, K. Allali. Mathematical Analysis of a SIHV COVID-19 Pandemic Model. In *Trends in Biomathematics: Stability and Oscillations in Environmental, Social, and Biological Models*, BIOMAT Consortium Lectures, Springer, Rio de Janeiro, Brazil, 2021. https://doi.org/10.1007/978-3-030-73241-7
25. A.A. Kilbas, H.M. Srivastava, J.J. Trujillo. *Theory and Applications of Fractional Differential Equations*. Elsevier, Amsterdam, 2006. ISBN: 978-0-444-51832-3.
26. J. LaSalle. Some extensions of Liapunov's second method. *IRE Trans. Circuit Theory*, 7(4), 520–527 (1960). https://doi.org/10.1109/TCT.1960.1086720
27. Z. Lu, Y. Yu, G. Ren, C. Xu, X. Meng. Global dynamics for a class of reaction–diffusion multigroup SIR epidemic models with time fractional-order derivatives. *Nonlinear Anal. Model. Control*, 27(1), 142–162 (2022). https://doi.org/10.15388/namc.2022.27.25192
28. F. Mansal, M.A.M.T. Balde, A.O. Bah. Optimal Control on a Mathematical Model of SIR and Application to Covid-19. *Biennale Des Mathématiques* (2023).
29. A. Meskaf, Y. Tabit, K. Allali. Global analysis of a HCV model with CTL, antibody responses and therapy. *Appl. Math. Sci.*, 9(81), 4025–4034 (2015). https://doi.org/10.12988/ams.2015.53139
30. N.A. Nayied, F.A. Shah, M.A. Khanday, K.S. Nisar. Numerical Investigation of Fractional Order SEIR Models with Newborn Immunization Using Vieta–Fibonacci Wavelets. *Partial Differ. Equ. Appl. Math.*, 12, 100995 (2024). https://doi.org/10.1016/j.padiff.2024.100995
31. K.S. Nisar, K. Logeswari, V. Vijayaraj, H.M. Baskonus, C. Ravichandran. Fractional Order Modeling the Gemini Virus in Capsicum Annuum with Optimal Control. *Fractal Fract.*, 6(2), 61 (2022). https://doi.org/10.3390/fractalfract6020061
32. I. Podlubny. *Fractional Differential Equations*. Academic Press, San Diego, CA, 1999. ISBN: 978-0-12-558840-9.
33. L.S. Pontryagin, V.G. Boltyanskii, R.V. Gamkrelidze, E. Mishchenko. *The Mathematical Theory of Optimal Processes*. Interscience, New York, 1962.
34. M.N.H. Qomarudin, W. Windarto, Z. Chazuka. Stability analysis of influenza virus spread model in bird population with reaction–diffusion. *Stat. Optim. Inf. Comput.*, 16(2), 1845–1864 (2026).
35. D. Rocha, C.J. Silva, D.F.M. Torres. Stability and optimal control of a delayed HIV model. *Math. Methods Appl. Sci.*, 40(17), 6263–6280 (2017). https://doi.org/10.1002/mma.4451
36. M. Sadki, J. Danane, K. Allali. Hepatitis C virus fractional-order model: mathematical analysis. *Model. Earth Syst. Environ.*, 9(2), 1695–1707 (2023). https://doi.org/10.1007/s40808-022-01582-5
37. M. Sadki, S. Harroudi, K. Allali. Dynamical analysis of an HCV model with cell-to-cell transmission and cure rate in the presence of adaptive immunity. *Math. Model. Comput.*, 9(3), 579–593 (2022). https://doi.org/10.23939/mmc2022.03.579
38. N.H. Sweilam, S.M. Al-Mekhlafi. Numerical study for multi-strain tuberculosis (TB) model of variable-order fractional derivatives. *J. Adv. Res.*, 7(2), 271–283 (2016).
39. M. Tafrikan, Fatmawati, Windarto, C.E. Madubueze. Fractional dynamics and sensitivity analysis of a diphtheria spread model. *Stat. Optim. Inf. Comput.* (in press).
40. C. Vargas-De-Leon. Volterra-type Lyapunov functions for fractional-order epidemic systems. *Commun. Nonlinear Sci. Numer. Simul.*, 24(1–3), 75–85 (2015).
41. Z. Yaagoub, J. Danane, K. Allali. Global Stability Analysis of Two-Strain SEIR Epidemic Model with Quarantine Strategy. In *Nonlinear Dynamics and Complexity: Mathematical Modelling of Real-World Problems*, pp. 469–493, Springer (2022). https://doi.org/10.1007/978-3-031-06632-0_22
42. Z. Yaagoub, M. Sadki, K. Allali. A generalized fractional hepatitis B virus infection model with both cell-to-cell and virus-to-cell transmissions. *Nonlinear Dyn.*, 112, 16559–16585 (2024). https://doi.org/10.1007/s11071-024-09867-3
43. Z. Yaagoub, M. Sadki, K. Allali. Global stability of spatio-temporal model with quarantine and vaccination. *J. Indones. Math. Soc.*, 30(2), 321–337 (2024). https://doi.org/10.22342/jims.30.2.1452.321-337
44. L. Zhang, Y. Liu, Y. Chen. Stability and bifurcation analysis of a multi-strain SEIR epidemic model with general incidence rates. *Appl. Math. Comput.*, 386, 125479 (2020).